

Novel Designs and simulations to fabricate Microbolometer sensor and Si microbridges using low cost approach

Radharamana Mohanty

A Dissertation Submitted to
Indian Institute of Technology Hyderabad
In Partial Fulfillment of the Requirements for
The Degree of Master of Technology



भारतीय प्रौद्योगिकी संस्थान हैदराबाद
Indian Institute of Technology Hyderabad

Department of Electrical Engineering

June, 2014

Declaration

I declare that this written submission represents my ideas in my own words, and where others' ideas or words have been included, I have adequately cited and referenced the original sources. I also declare that I have adhered to all principles of academic honesty and integrity and have not misrepresented or fabricated or falsified any idea/data/fact/source in my submission. I understand that any violation of the above will be a cause for disciplinary action by the Institute and can also evoke penal action from the sources that have thus not been properly cited, or from whom proper permission has not been taken when needed.

(Signature)

(Radharamana Mohanty)

(Roll No)

Approval Sheet

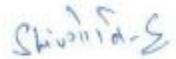
This thesis entitled Innovative technique to Fabricate Microbolometer Sensor and Si Microbridges/Cantilevers by Radharamana Mohanty is approved for the degree of Master of Technology from IIT Hyderabad.



Examiner



Examiner



Adviser

(for Sira Vanjari) 

Co-Adviser



Chairman

Acknowledgements

First of all I want to acknowledge Dr. Shiv Govind Singh sir for his consistent guidance, support and help. All the transparent discussions and philosophies were very helpful to me.

I am willing to thank Dr. Asudeb Dutta sir and Dr. Siva Rama Krishna sir for helping me with their research experience.

I am also grateful to Tamal Ghose and Durga Prakash for helping me through out in my project.

I am thankful to chanda karthik for his support in this project.

Finally, I want to thank my friends Manas, Ghanashyam, Nagveni, Meher, Jitendra, Rohit, Pramod , Roopak and all my juniors for making my stay in IITH so special and wonderful.

Dedicated to

My Family and friends.....

Abstract

Frontend bulk micro machining is one of the proven techniques of making suspended microstructures and is highly adapted due to its simple and cost effective way of fabricating the devices. We propose novel geometric mask designs for achieving area efficient microstructures by frontend Si bulk micromachining.

In this work we adapt the geometric mask design having a microstructure between two rectangular openings. These openings are aligned at 45° to wafer prime flat of (100) silicon wafer and act as etch openings for frontend bulk micromachining. However rectangular openings lead to high silicon area consumption which makes the process unworthy. Therefore we proposed different geometries to minimize area consumption for achieving the same dimension of suspended structure. All these different geometries are simulated using Intellisuite FABSIM based physical simulator. We have observed more than 28% reduction in foot print over literature reported design.

Here also we are reporting the development of low-cost uncooled infrared microbolometer detector, Where the Si itself is used as the infrared sensitive material. The process does not required any diffusion or electrochemical etch-stop technique as is required in traditional CMOS line microbolometer fabrication, rather we are reporting two ways of fabricating the device in which one of the fabrication is done by using only one mask with only front end bulk micro machining using anisotropic and isotropic wet etchants which minimizes the fabrication cost of the device drastically.

Contents

Declaration.....	ii
Approval Sheet.....	Error! Bookmark not defined.
Acknowledgements	iv
Abstract.....	vi
Chapter 1 Introduction	1
1.1 Infrared and Infrared Detection.....	Error! Bookmark not defined.
1.2 Motivation	3
1.3 Aim and Objective of Thesis	5
1.4 Thesis Outline.....	5
Chapter 2 Literature Survey	7
2.1 Fabrication of Si Microbriges and Cantilevers	7
2.2 Microbolometer and Fabrication	8
Chapter 3 Electrochemical Wet etching.....	11
3.1 Electrochemical etch stop technique.....	11
3.2 Electrochemical Etch stop Setup.....	11
3.3 Proposed Method to make Si Microbridges.....	13
3.4 Issues in the Proposed Method.....	16
Chapter 4 Non electrochemical Method for Si microbridges	17
4.1 Proposed method for making Si microbridges.....	17
4.2 Mathematical Calculations for Microbridge.....	20
4.3 Issues in Proposed Method.....	21
Chapter 5 Silicon Bulk Micromachining	22
5.1 Frontend Bulk micromachining to Make Si microbridges.....	22

5.2	Process flow to obtain Si Microbridge.....	24
5.3	Result and Discussion.....	26
Chapter 6 Simulation and Fabrication of Si Microbridges.....		29
6.1	Proposed Method to reduce area consumption for making Si Microbridges.....	29
6.2	Simulation and Fabrication of Area efficient Si microbridges.....	30
6.3	Comparative case study of the all area efficient mask Designs.....	33
Chapter 7 Microbolometer and design.....		34
7.1	Innovative methods for Fabricating Microbolometer	34
7.2	Process Simulation showing Microbolometer Fabrication using only Front end Bulk micromaching	35
7.2.1	Only using wet etching.....	35
7.2.1.1	Simulation Results.....	36
7.2.2	Dry etching followed by Wet etching.....	37
7.2.2.1	DRIE followed by TMAH etching.....	37
7.2.2.1.1	Simulation Results.....	39
7.2.2.2	DRIE followed by HNA etching.....	39
7.2.2.2.1	Simulation Results.....	40
Chapter 8 Efficient Method to Fabricate Microbolometer.....		41
8.1	Design and Simulation of area efficient Microbolometers	41
8.1.1	Only using wet etching.....	42
8.1.2	Dry etching followed by Wet etching.....	45
8.1.2.1	DRIE followed by TMAH etching.....	45
8.1.2.2	DRIE followed by HNA etching.....	48
Chapter 9 Comparative Case study of Making Microbolometer Sensor.....		51
9.1	Comparisons between only wet etching and dry followed by wet etching.....	51
9.2	Comparisons between sub methods under method-2.....	52

9.3	Comparisons between proposed methods and existing methods of making microbolometer sensor.....	53
Chapter 10	Conclusion and Future Work.....	54
10.1	Conclusion.....	54
10.2	Future Scope of Work.....	54
References.....		55

Chapter 1

Introduction

1.1 Infrared and Infrared Detection

Infrared (IR) is electromagnetic radiation with longer wavelengths than those of visible light, extending from the nominal red edge of the visible spectrum at 700 nanometers (nm) to 1 mm. Infrared radiation was discovered in 1800 by astronomer William Herschel, who discovered a type of invisible radiation in the spectrum beyond red light, by means of its effect upon a thermometer. Most of the thermal radiation emitted by objects near room temperature is infrared. Infrared radiation can be used to remotely determine the temperature of objects (if the emissivity is known), this is termed thermography.

Thermographic cameras detect radiation in the infrared range of the electromagnetic spectrum (roughly 9,000–14,000 nanometers or 9–14 μm) and produce images of that radiation, called thermograms. Since infrared radiation is emitted by all objects above absolute zero according to the black body radiation law, thermography makes it possible to see one's environment with or without visible illumination. The amount of radiation emitted by an object increases with temperature; therefore, thermography allows one to see variations in temperature. When viewed through a thermal imaging camera, warm objects stand out well against cooler backgrounds; humans and other warm-blooded animals become easily visible against the environment, day or night. As a result, thermography is particularly useful to military and other users of surveillance cameras. Specialized thermal imaging cameras use focal plane arrays (FPAs) that respond to longer wavelengths (mid- and long-wavelength infrared). The most common types are InSb, InGaAs, HgCdTe and QWIP FPA. The newest technologies use low-cost, uncooled microbolometers as FPA sensors. Their resolution is considerably lower than that of optical cameras, mostly 160x120 or 320x240 pixels, up to 640x512 for the most expensive models. Thermal imaging cameras are much more expensive than their visible-

spectrum counterparts, and higher-end models are often export-restricted due to the military uses for this technology. Older bolometers or more sensitive models such as InSb require cryogenic cooling, usually by a miniature Stirling cycle refrigerator or liquid nitrogen.

A bolometer is a device for measuring the power of incident electromagnetic radiation via the heating of a material with a temperature-dependent electrical resistance. It was invented in 1878 by the American astronomer Samuel Pierpont Langley. The name comes from the Greek word *bole* (βολή), for something thrown, as with a ray of light. Langley's bolometer consisted of two platinum strips covered with lampblack. One strip was shielded from radiation and one exposed to it. The strips formed two branches of a Wheatstone bridge which was fitted with a sensitive galvanometer and connected to a battery. So when resistance of the exposed platinum gets changed there will be current flow in the galvanometer.

A microbolometer is a specific type of bolometer used as a detector in a thermal camera. Infrared radiation with wavelengths between 7.5-14 μm strikes the detector material, heating it, and thus changing its electrical resistance. This resistance change is measured and processed into temperatures which can be used to create an image. Unlike other types of infrared detecting equipment, microbolometers do not require cooling.

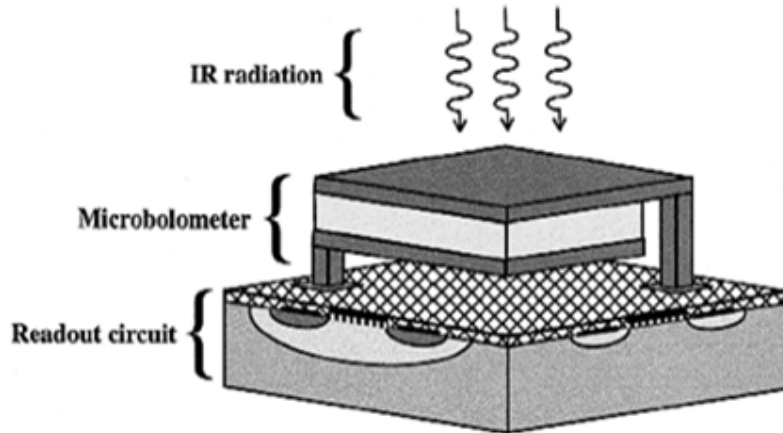


Fig.1.1: Microbolometer and Readout Circuit.

As shown above the fig.1.1 shows the microbolometer with its corresponding ROIC as a complete system.

1.2 Motivation

An infrared sensor is an electronic instrument that is used to sense certain characteristics of its surroundings by either emitting and/or detecting infrared radiation. It is also capable of measuring heat of an object and detecting motion. The IR sensor has verity of applications as mentioned below

- Tracking and art history.
- Climatology, meteorology, and astronomy.
- Thermography, communications, and alcohol testing.
- Heating, hyperspectral imaging, and night vision.
- Biological systems, photobiomodulation, and plant health.
- Gas detectors/gas leak detection.
- Water and steel analysis, flame detection.
- Anesthesiology testing and spectroscopy.
- Petroleum exploration and underground solution.
- Rail safety.

Below shows some pictures taken by microbolometer sensors and their field of applications.

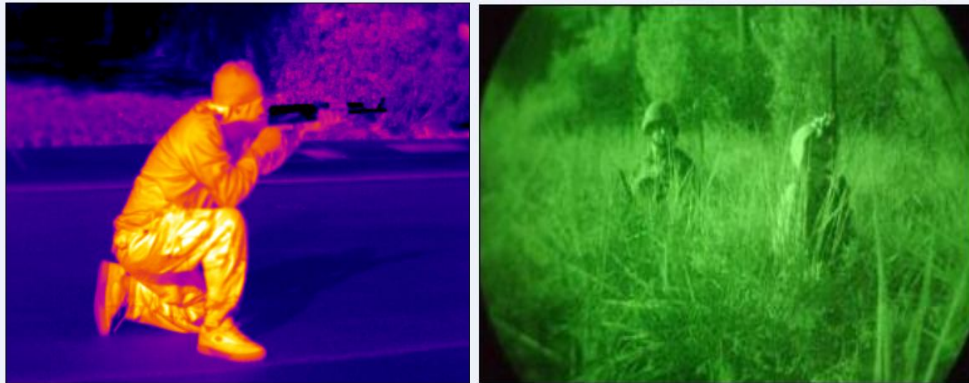


Fig1.2: Night vision mainly used in military.

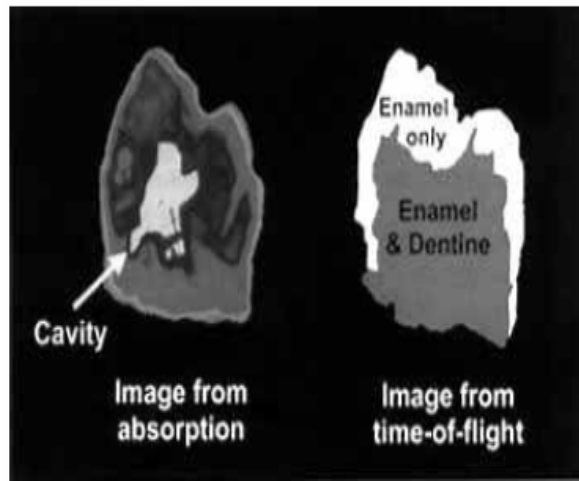


Fig.1.3: Early detection of tooth cavity.

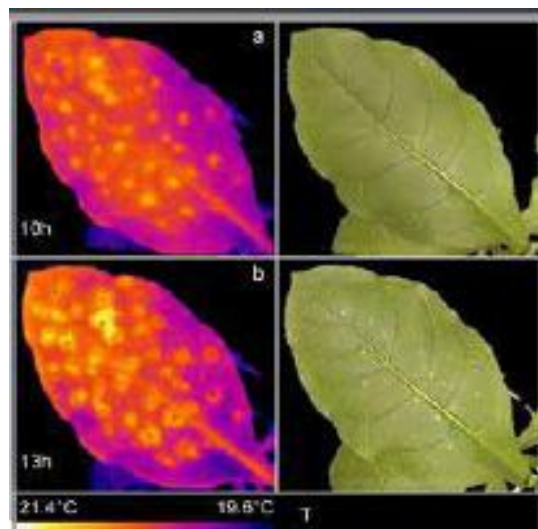


Fig.1.4: Determining net water loss

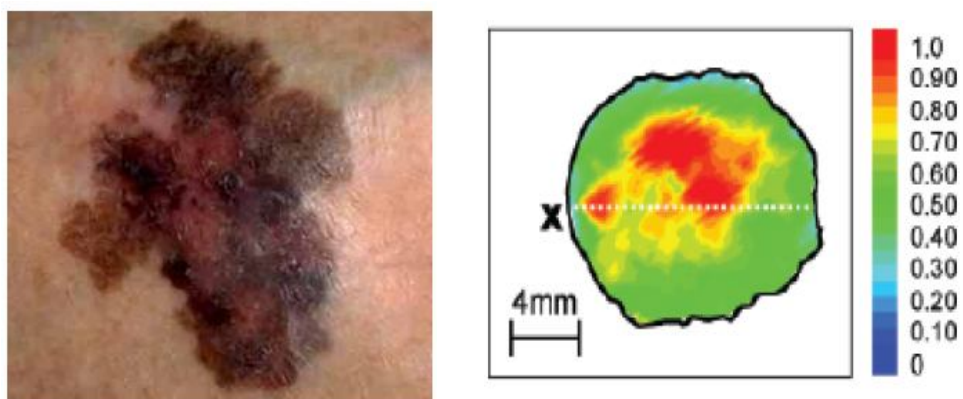


Fig.1.5: Detection of skin cancer

As mentioned above the IR sensor/detector is used in many fields of applications. Hence the quality of image, sensitivity of the device and cost play very important role in different field of applications. For example in astronomy the sensitivity of the device matters more as it has to detect asteroids from distance places but in biomedical applications rather than sensitivity cost matters a lot.

1.3 Aim and objectives of the thesis

Main objective of the thesis was to make the commercial based IR sensor, microbolometer in ultra-low cost and simple method of fabrication. Our aim was firstly to make the Microbolometer sensing element using simple process steps and then go for 3D integration of the sensor with its corresponding ROIC, so that the sensing membrane with its ROIC can be available as a complete package. This will be of low cost and efficient IR sensor with considerable reduced effort. While making the microbolometer sensor we also designed Si based microbridges/cantilevers using low cost and simple etching steps.

1.4 Thesis Outline

Before going for bolometer fabrication we targeted to 1st fabricate a simple Si cantilever/microbridge structure which could be the basic structure for the bolometer to fabricate. We started with the traditional electrochemical wet etching process to fabricate the Si microbridges and end up with novel idea to fabricate Si microbridges, which was low cost method to fabricate microbridges. Then we used this technique and tried to fabricate the microbolometer structure which is also of low cost.

So the outline of the thesis comprises of two distinct sections one in which we have developed efficient Si microbridges and second in which we have developed efficient microbolometer sensors. The detail of the work is put in the chapters shown below which is explained completely in later stages.

- I. Electrochemical etch stop method to fabricate Si Microbridges and the issues associated.
- II. Non-electrochemical etches stop method to fabricate Si micro bridges and the issues associated.

- III. Design, Simulation and fabrication of Si based Microbridges/cantilever and array using front end bulk micromachining.
- IV. Design optimization by making efficient mask designs to reduce area consumed per microbridge and increase in number of microbridges.
- V. A comparative case study to make Si microbridges using all of the above designs and hence showing the most optimized mask design in fabricating microbridges and micro cantilevers both in terms of area utilization and number of devices.
- VI. Design and Simulation of Microbolometer sensors using two methods
 - 1. Using only wet etching.
 - 2. Using Dry etching followed by wet etching.
 - DRIE followed by TMAH etching.
 - DRIE followed by HNA etching.
- VII. A comparative case study between the above mentioned methods of fabricating microbolometer.
- VIII. Design optimization by making efficient mask designs to reduce area consumed per pixel of microbolometer.
- IX. A comparative case study of area efficient mask designs to make microbolometer.

The detail of the thesis outline presented above is explained in the next chapter with the results.

Chapter 2

LITERATURE SURVEY

2.1 Fabrication of Si Microbridges and Cantilevers

Micro-electro-mechanical systems (MEMS) consist of mechanical components as well as electronic circuits integrated with each other as a complete system. Micro fabrication plays a very important role in miniaturizing the mechanical components as a result of which those devices are capable of integrated with electronics which as a whole system can be implemented in chip giving very good performance. Surface and bulk micromachining [1] are the two most important processes to make mechanical components. Being simple and cost effective way of removing parts of Silicon, anisotropic wet etching is highly demanded in MEMS processes to make different types of sensors and actuators.

Microcantilevers and microbridges are the frequently used structures in many of MEMS devices and except that simple structures are also used as thermal, mechanical and biomolecule detectors. So the ease and cost of process is highly dependent of the fabrication of those microstructures. There are majorly three methods to fabricate Si Microbridges/cantilevers.

- i. By using a sacrificial layer.
- ii. SOI method.
- iii. Bulk micromachining.

Using a sacrificial layer for making the device causes the ease of fabrication difficult similarly using an SOI wafer makes the cost of the process high. But bulk micromachining of Si to make the microbridge/cantilever is one of the simple and cost effective ways to fabricate the microbridges/cantilevers.

2.2 Microbolometer and Fabrication

Bolometers are nothing but the Heat or IR sensors in which basically the resistance of the device get changed with the absorbed IR radiation. Every living and non-living objects have certain thermal signature, the device is able to detect the object from the IR radiation emitting from it. Hence it has a wide range of applications such as night vision, infrared imaging, biomedical applications such as skin cancer, early tooth cavity detection except these it also used in astronomy and so on. Microbolometers are getting more attention because of its light weight, low cost and low power usage. But the challenge lying in implementing very large format arrays at low cost.

A lot of techniques have been reported so far to fabricate microbolometers and array of it [2]. The most commonly used manufacturing approach for uncooled infrared bolometer FPAs is monolithic integration, which is shown below.

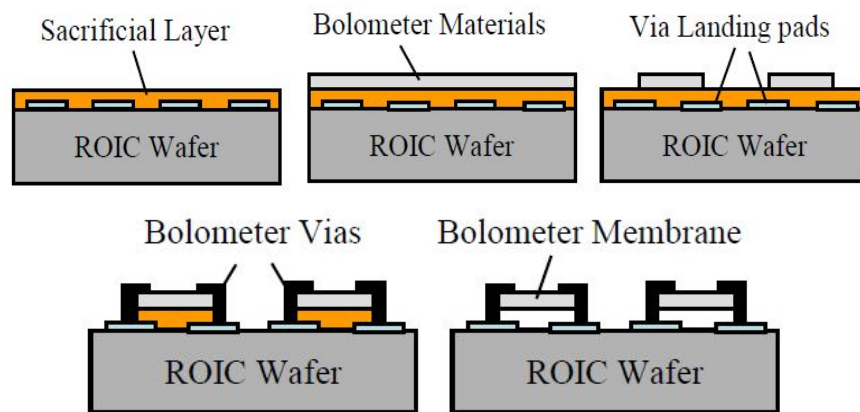


Fig2.1: showing monolithic method of bolometer fabrication

In this method ROIC is pre-manufactured then on top of that a high temperature polyamide is deposited as sacrificial layer. The bolometer material (ex. VOx) is deposited on top of that which is then patterned and bolometer vias are created for contact, then by using oxygen plasma the sacrificial layer is removed which results in free isolated bolometer.

But the disadvantages we observed in this method are

- (1) Some monocrystalline bolometer materials require more than 450 degree centigrade for deposition which may damage our underlying ROIC at that temperature.
- (2) As the structure obtained in this method is hanging without any support so the reliability is the major concern in this method.

The second method of fabrication is the bulk micromachining the fabrication is done in CMOS line after the ROIC is made shown in fig.2.2 [3, 4]. In this method of fabrication

electrochemical etch stopping technique [5] is used for which there require n-well layers in p-type substrate and those n-wells are used as the sensing elements.fig.2.2 shows the bolometer device obtained using bulk micromachining.

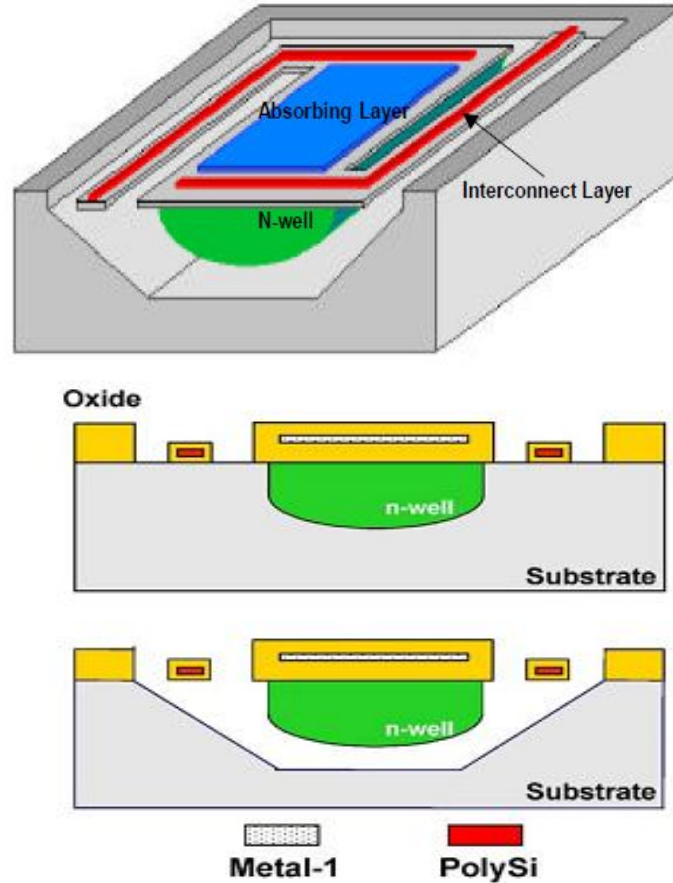


Fig.2.2: showing the front view of CMOS line microbolometer

In this method the bolometer is fabricated in standard CMOS line i.e. first the ROIC is fabricated and after that bulk micromachining is done by electrochemical etching method where an n-well is used as the etch stop layer.

But the disadvantages got in this method are

- (1) The ROIC cannot place beneath the bolometer membrane which reduces the pixel form factor.
- (2) The end step is the electrochemical wet etching step which required potential to apply for the etching to be stopped in sensor membrane which is cumbersome while going for array of bolometers and may not good for the ROIC.

Then the third important method to fabricate microbolometer is 3D integration [6], which avoids the high temperature issue in monolithic for which it was difficult to put some monocrystalline material on top of ROIC wafer. The process steps are shown in fig.2.3.

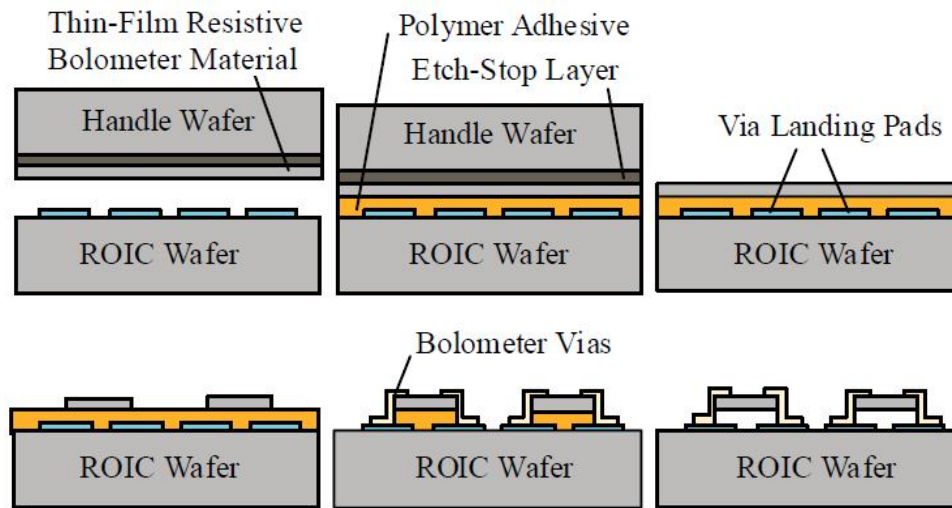


Fig.2.3: showing heterogeneous 3D integration of bolometer

But the issues laying in the above method are

- (1) Still the method suffers from reliability issue.
- (2)The process is costly as it requires a handle wafer which is normally SOI.

There are a lot of materials proposed to be used as the bolometer material few of which with their temperature coefficient of resistance is put here.

Table-2.1 showing bolometer material with its TCR

Bolometer Material	Temp. coefficient of Resistance(TCR)
VOx	3% /°k
Amorphous Si(α -Si)	3% /°k
Amorphous Si thin film transistor(TFT)	1.5-6.5%/°k
Titanium	0.35%/°k
Germanium-silicon-oxygen compounds ($G_xSi_{1-x}O_y$)	5.1%/°k

Chapter 3

Electrochemical Wet Etching

3.1 Electrochemical etch stop technique

It is one of the important technique to manufacture microstructures such as cantilevers, micro bridges etc. In this technique there required a reverse biased p-n junction which prevents etching leading to formation of free isolated micro structures. This technique was first proposed by Waggener. In this technique at first an n-type epitaxial layer is formed over the p-type substrate by doping and a thick thermal oxide is grown on top of it which acts as an etch mask in wet etchant KOH. Then the oxide is patterned to expose the area to be etched in the substrate. Then a positive voltage is applied to the n-epilayer through ohmic contact and an electrical contact is established in p-substrate through the etch solution using a counter electrode. Under sufficient anodic biases silicon passivates and oxide grows over n-epilayer as a result etch stops. Since majority of the potential drops across the reverse biased p-n junction the p-type silicon (substrate) remains at the open circuit potential (OCP) and etches. But the complete removal of substrate from n-epilayer will expose the epilayer to the solution. The positive potential applied to the n-layer then passivates it and etch stops [7,8,9].

3.2 Electrochemical Etch stop setup

The electrochemical etch setup to achieve this is as shown in the fig.3.1. Below Setup shown is four electrode wet etch stop setup.

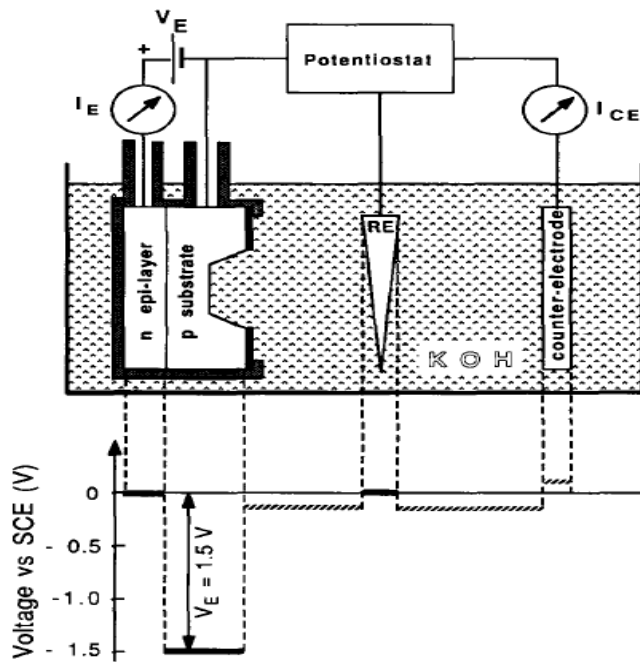
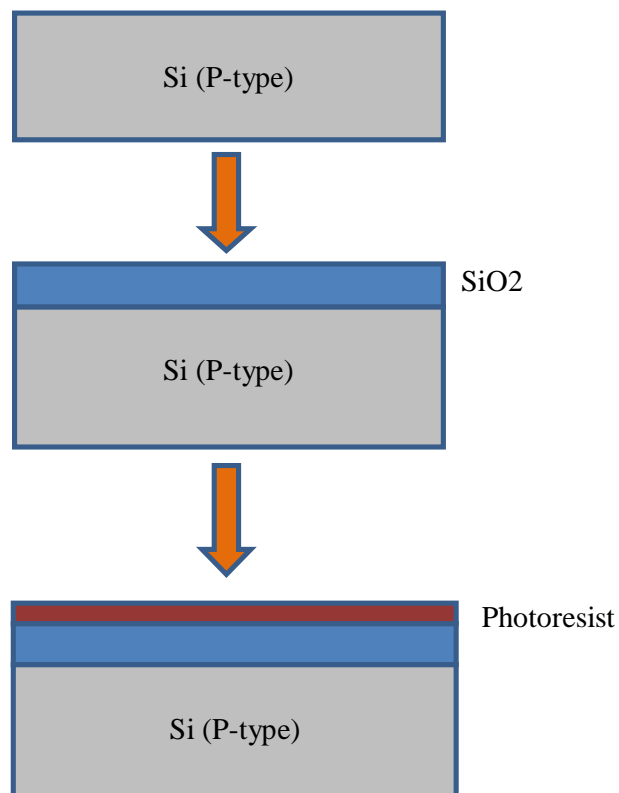
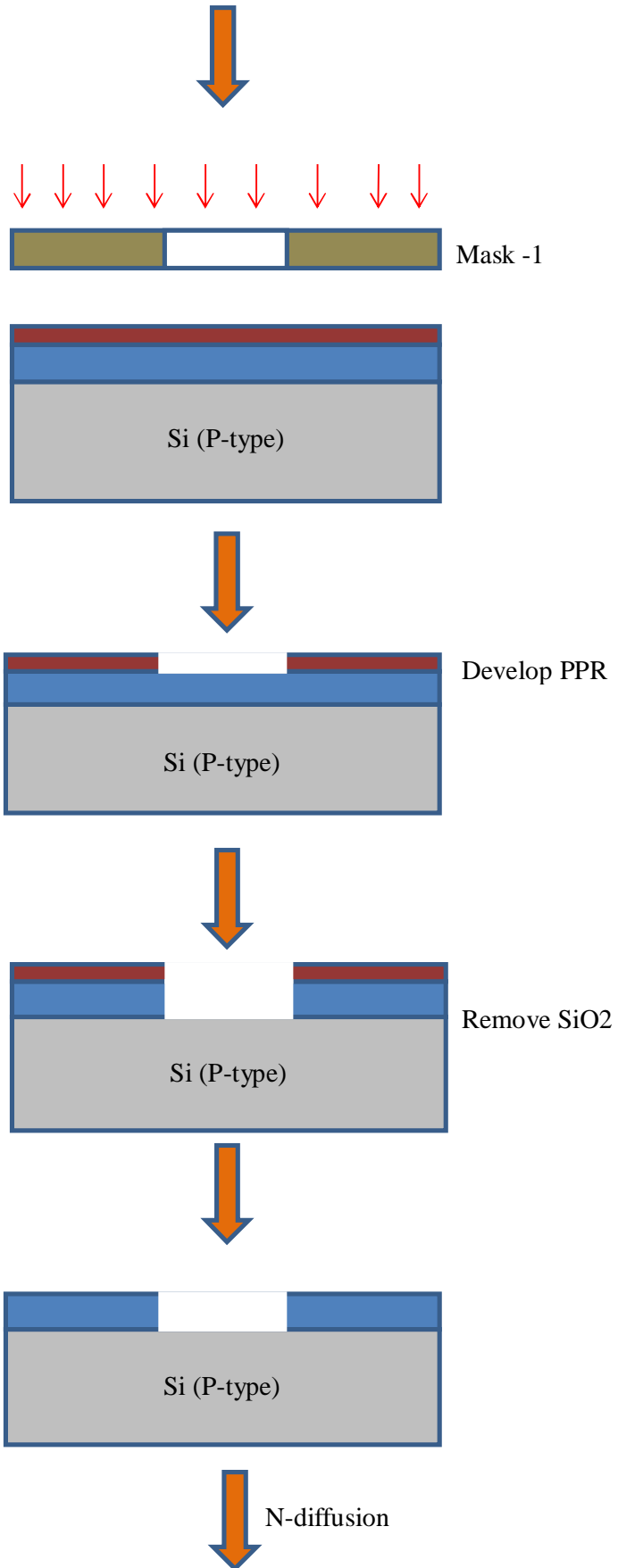


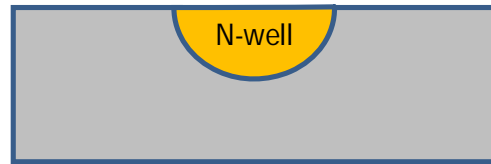
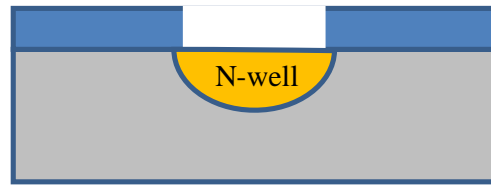
Fig.3.1: showing Four electrode electrochemical etch stop configuration. Si microbridge formation.

3.3 Process flow for Making Si Microbridges

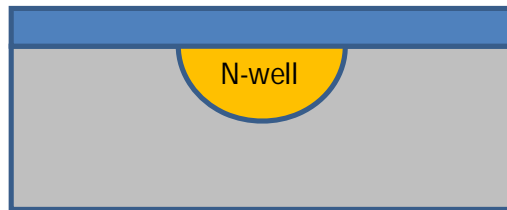
Using the above mentioned electrochemical etch stopping technique we tried to fabricate Si microbridge. Below shows the process steps to fabricate it.



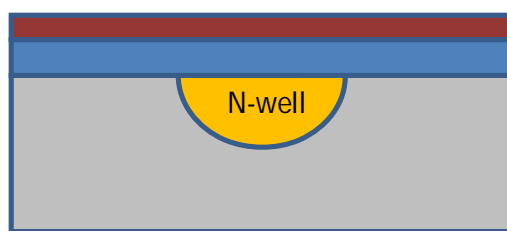




Remove SiO₂



Grow SiO₂ on entire surface



Spun ppr



MASK-2

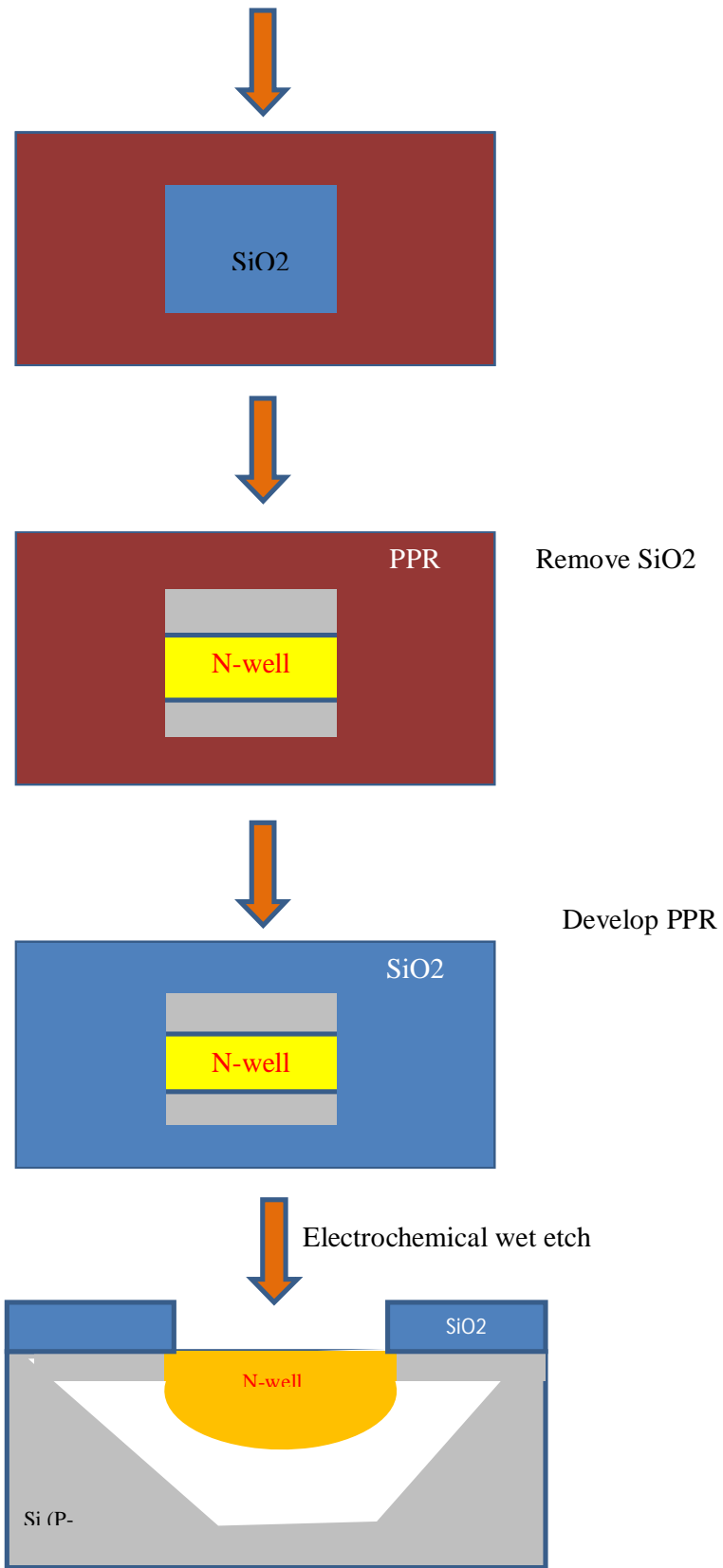


Fig.3.2 showing the process steps to obtain Si microbridge.

3.4 Issues in the present method

The present method is not new in making Si microbridges. But we did not find it convenient while building this set up. These are the few issues we faced in the technique.

- Giving an ohmic contact and putting in KOH solution was found to be difficult.
- A particular potential has to be applied for proper operation which was found to be difficult.
- Making ohmic contact for array of devices was found to be difficult.

So we thought of going some easy way of fabricating microbridges which will not require those cumbersome process.

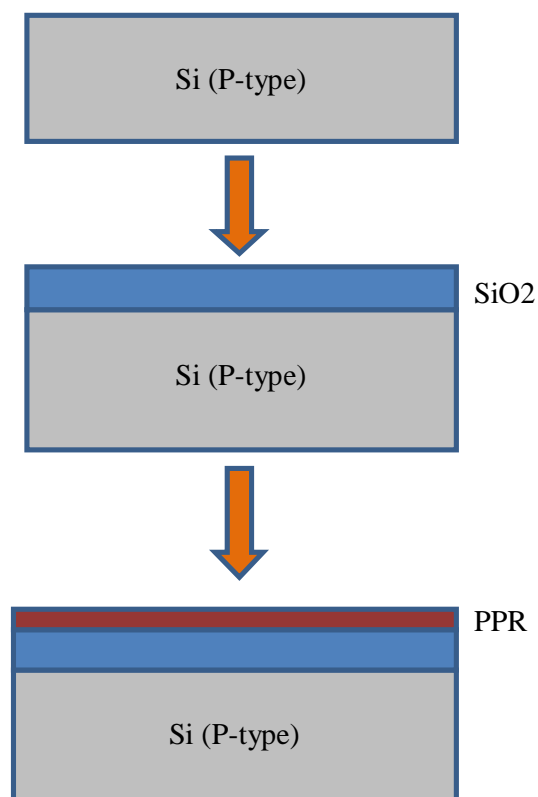
Chapter 4

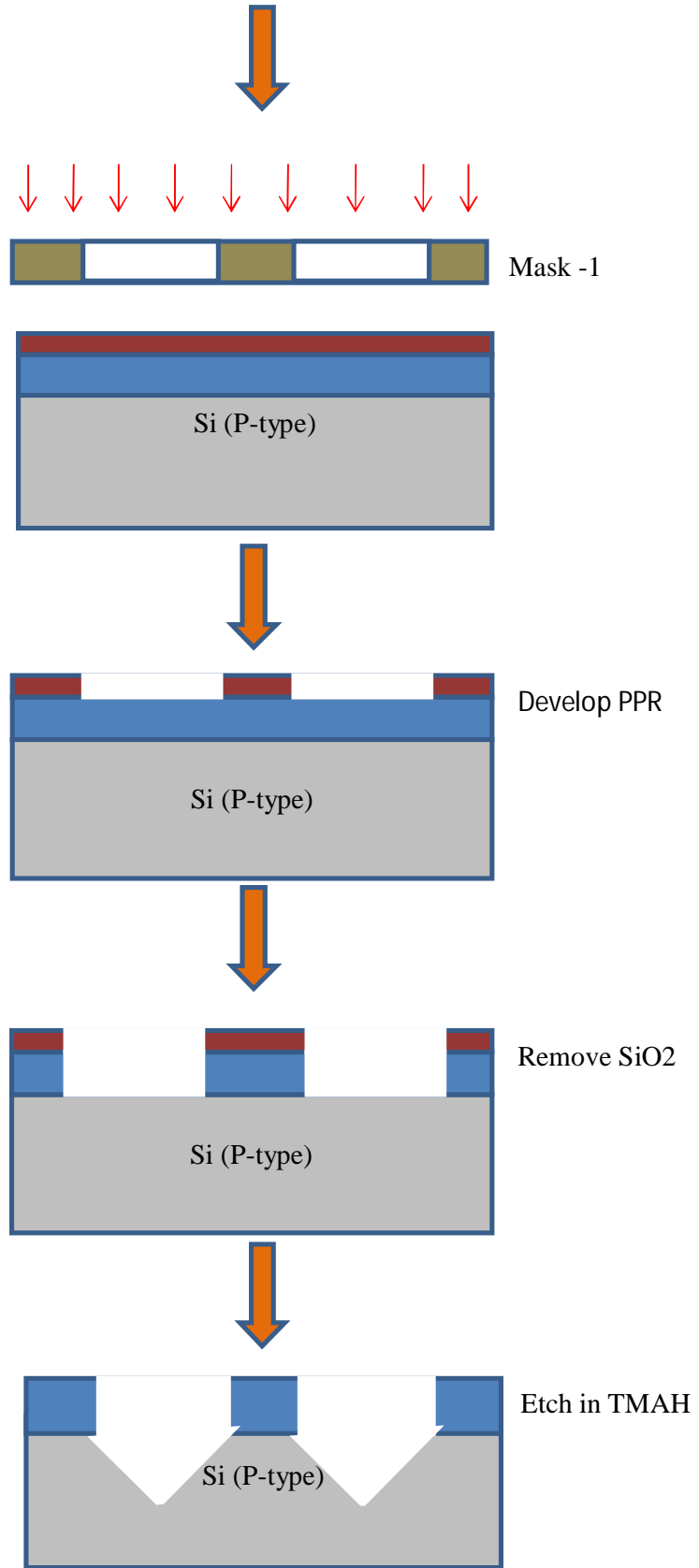
Non electrochemical etch stop method to make Si micro bridges

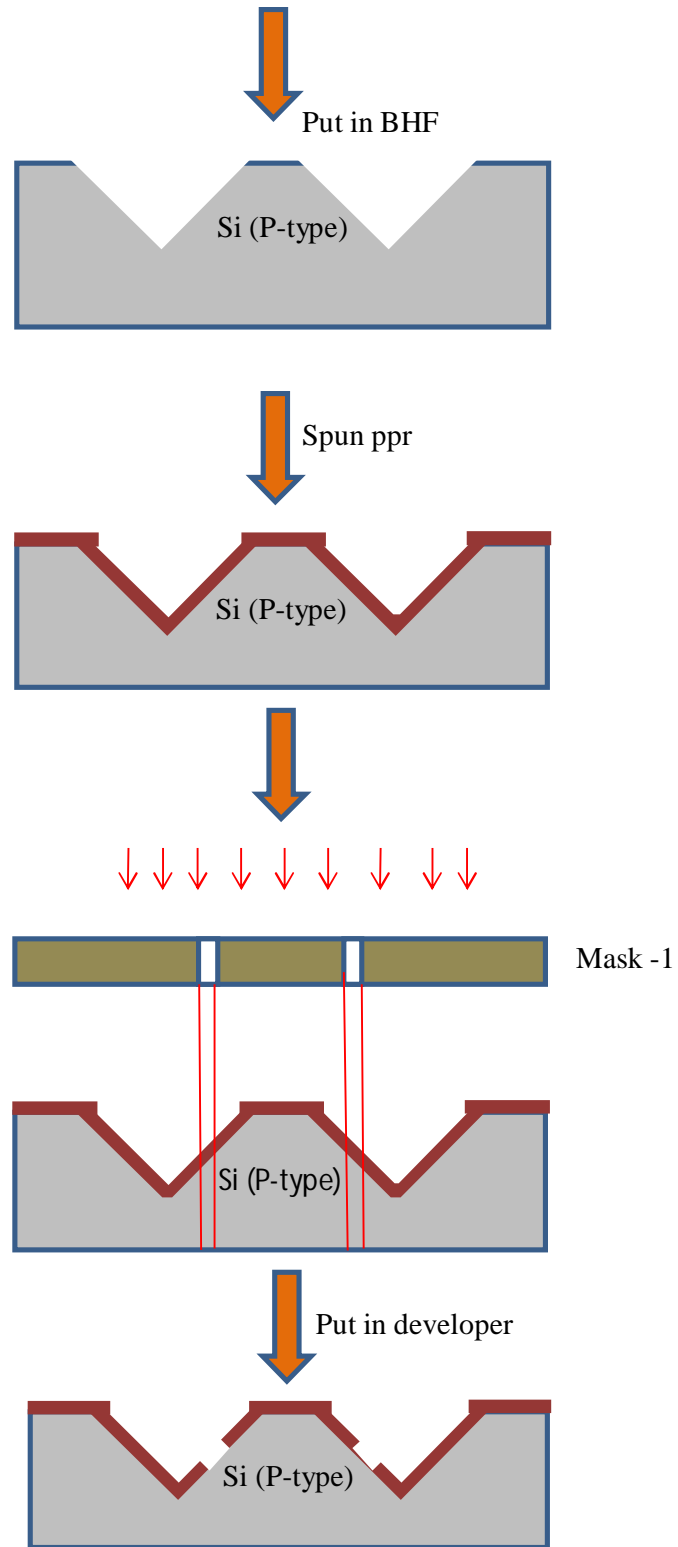
4.1 Proposed Method for making silicon microbridges

To make the process simple we planned to go for only bulk micromachining which will not require anything except chemical etching. We thought of two process to achieve this one is presented here and the second is presented in the next chapter.

The process was started with p-type <100> oriented wafer, where we created two openings and etched in TMAH. The etch pattern generated will make 54.7° to the horizontal and that is due to the exposure of <111> plane in that direction. In the next step we tried to break the <111> plane by putting in HNA and then carried TMAH etching which will result in a free hanging structure which is as shown below.







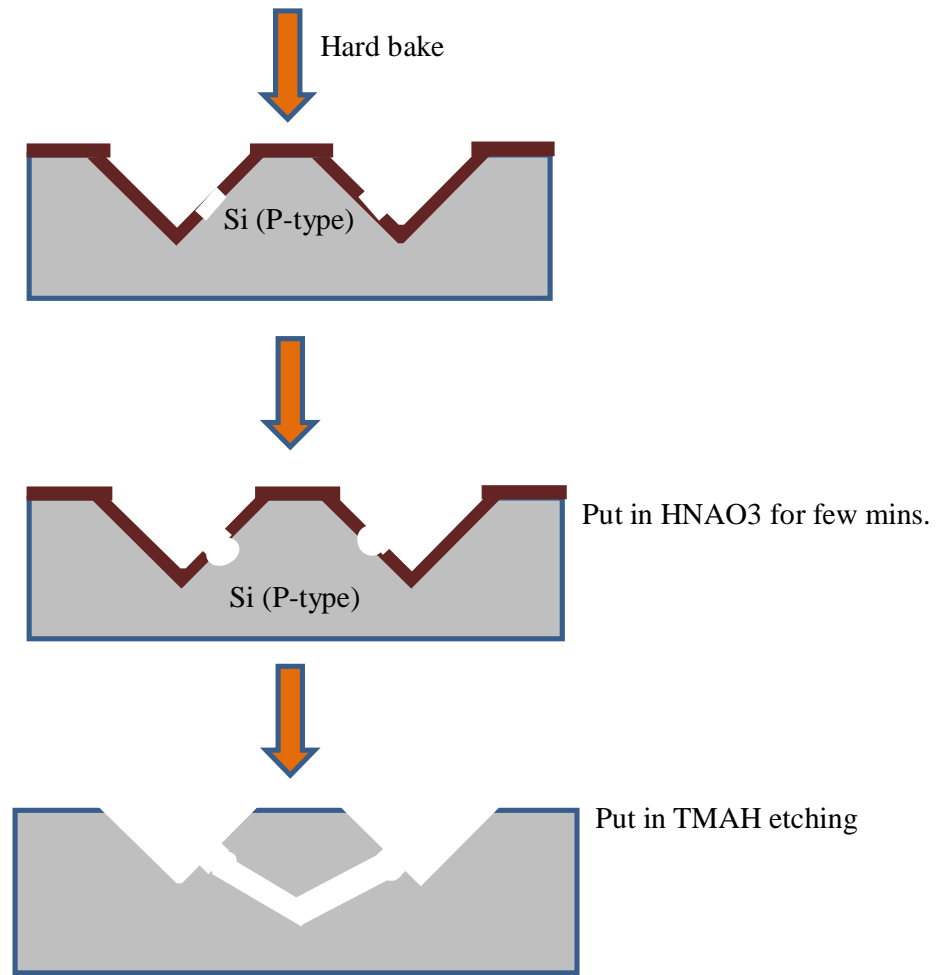


Fig.4.1 showing process flow for achieving Si microbridge

4.2 Mathematical Calculations for Si Microbridge

Below fig. shows a typical etching pattern obtained after 1st etching step for rectangular openings on Si surface. As shown we have created two mask openings in Si surface of width $200\mu\text{m}$ at a distance of $100\mu\text{m}$. TMAH was used for chemical etching. As the mask is creating rectangular opening to the wafer flat on Si surface, so it will create etch pattern that will aligned at 54.7° degree as shown. Due to this etching pattern the two $\langle 111 \rangle$ planes that makes the mentioned angle will meet at a point, giving V-groove structure. The depth of which will be around $143.234\mu\text{m}$ and the sides of the groove will be around $173.059\mu\text{m}$.

In the next step by using another mask we are trying to create openings in the V-groove as shown in the fig. For that we have used mask width of $50\mu\text{m}$ at a distance of $25\mu\text{m}$ from center of the groove. The mask will create an opening of around $86.53\mu\text{m}$ on the Si surface. Then we broke the V-groove to create an opening for TMAH opening and etched.

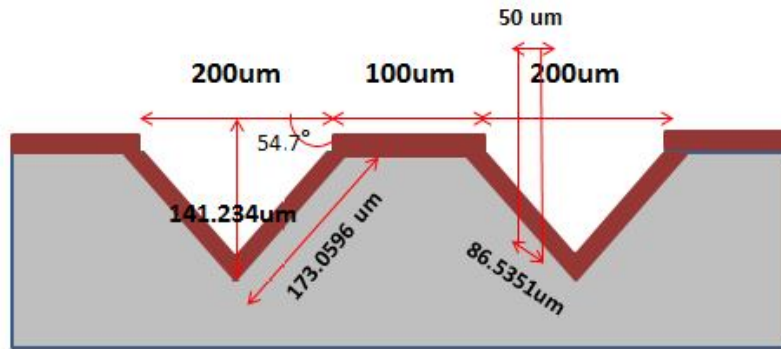


Fig.4.2 Showing calculations for mask opening

4.3 Issues in the method

There are few issues in the presented technique which are listed below.

- We cannot comment on the etched Si microbridge obtained i.e. how will be the structure look like. Because the shape of the microbridge depends on the exposed planes obtained after HNA etch.
- As we will go for smaller dimensions of Si microbridges miss alignment will create a big problem because if alignment will not proper then etching may not happen in the slanted wall got after 1st TMAH etching step due to which we may not give microbridge at all.

So we think of going even some more simple process to obtain Si microbridges which is explained in the next chapter.

Chapter 5

Silicon Bulk micromachining

5.1 Frontend Bulk micromachining to make Si microbridges

Frontend bulk micro machining is one of the proven techniques of making suspended microstructures and is highly adapted due to its simple and cost effective way of fabricating the devices. Here we propose novel geometric mask designs for achieving area efficient microstructures by frontend Si bulk micromachining.

In this work we adapt the geometric mask design having a microstructure between two rectangular openings. These openings are aligned at 45° to wafer prime flat of (100) silicon wafer and act as etch openings for frontend bulk micromachining. Alignment of the mask patterns relative to wafer crystallographic orientation is critical in the fabrication of many MEMS devices.

Etch rate of anisotropic wet etchant varies depending on the crystal plane exposed. Etch rate is lower on more densely packed surface than that of loosely packed surface so etch rate of $(100) > (110) > (111)$. The structure and dimension of the pattern etched on Si substrate depends not only on the orientation of Si substrate but also on geometry of opening, its alignment relative to wafer's crystal axes and the duration of etching [10]. Fig.5.1 shows the Si wet etch in (100) wafer where the mask is aligned in $\langle 110 \rangle$ direction. As shown the etched pattern obtained is bounded by four $\langle 111 \rangle$ planes and all those four planes make an angle of 54.7 degree with respect to the surface plane. But if we make the mask aligned in the $\langle 100 \rangle$ direction in (100) wafer then there can be seen significant undercut inside the mask layer. Si is not only etched in vertical direction but also etched in horizontal direction as all of the exposed planes are $\langle 100 \rangle$ in nature[11]. Fig.5.2 shows the etching in (100) wafer where mask oriented in $\langle 100 \rangle$ direction.

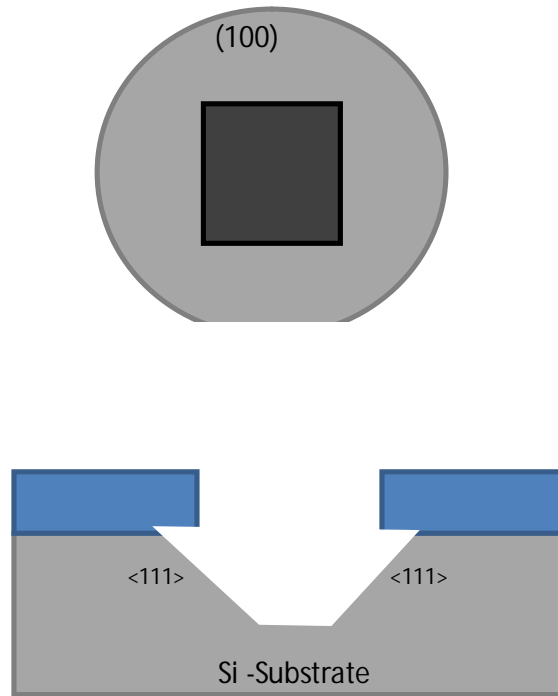


Fig.5.1: showing etching in <100> plane with the shown mask orientation with respect to wafer flat.

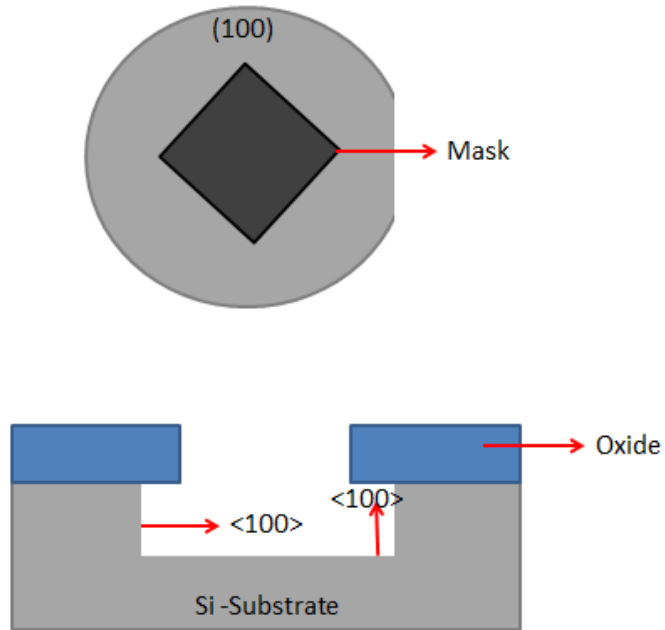
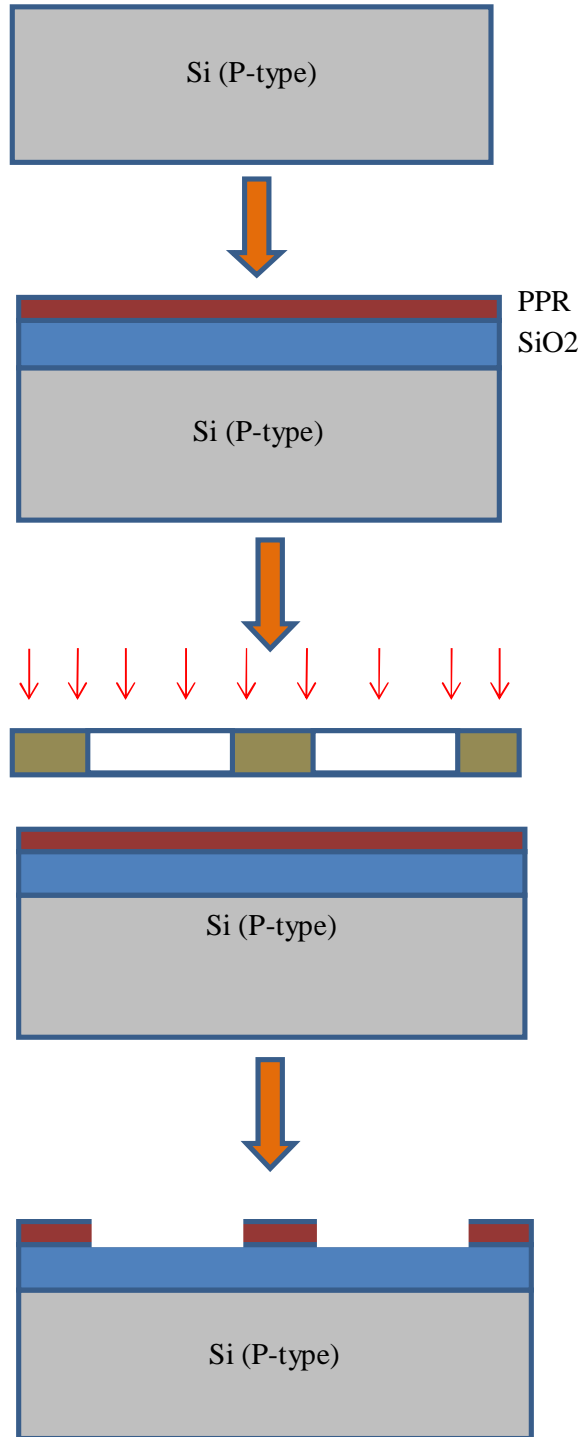
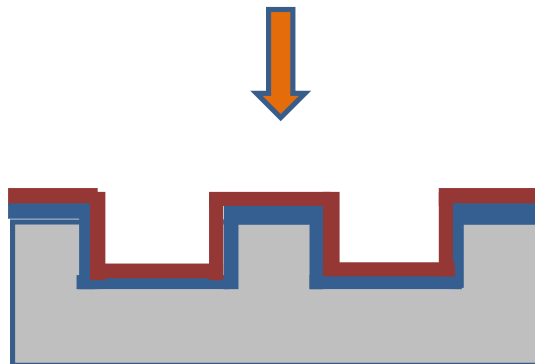
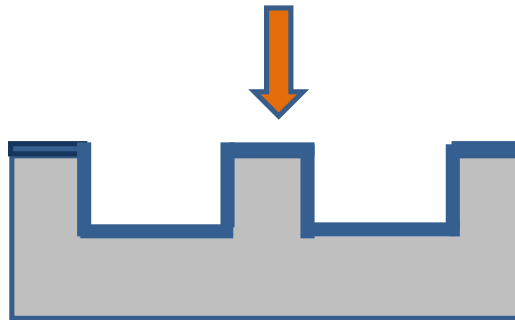
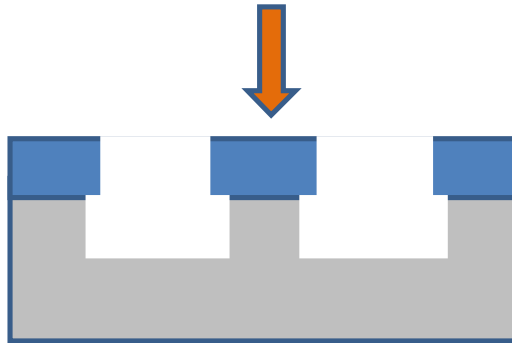
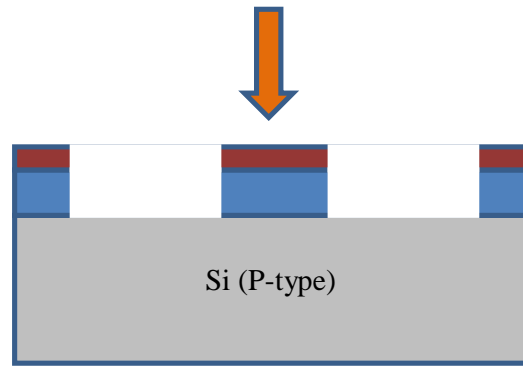


Fig. 5.2: Etched pattern obtained in (100) Si wafer with mask aligned in <100> direction.

5.2 Process flow for obtaining Si microbridge

The process flow for making the cantilevers is as shown below.





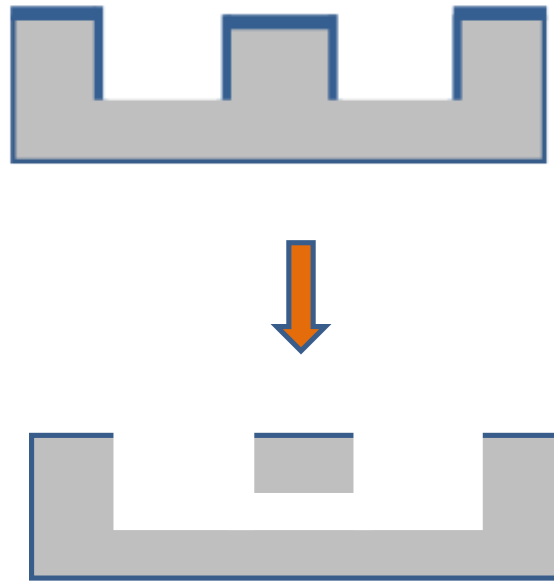


Fig.5.3: Process flow for making Si Bridge.

5.3 Results and Discussion

We made the desired mask and carried out the experiment to see the etched profile obtained in (100) wafer, when the mask is in $\langle 100 \rangle$ direction. Fig.5.4 shows wafer after 1st etching step and fig.5.5 and fig.5.6 shows optical profilometric images showing the plot of height versus width of the etched pillar obtained after the first etching. If the etching is done in both the direction then by controlling the time of etching and hence etches depth we can have Si cantilevers and bridges in only two step etching process but we need to protect the sidewalls of the etched pillars after first etching step.

We started the process with taking Si (100) wafer, oxidized it where the oxide acts as the etch mask. Made the mask and rotated it by 45° so that while exposing the mask will be in the direction of $\langle 100 \rangle$ plane. Then by using anisotropic etchant TMAH we etched the Si to the depth of 8 μ m. In the subsequent step we cleaned the etched wafer oxidised it. Using the same mask once again we exposed and etched to a depth of 16 μ m which results in the formation of Si cantilever/Bridge. The above process is simulated in FABSIM which is shown in Fig. 5.7.

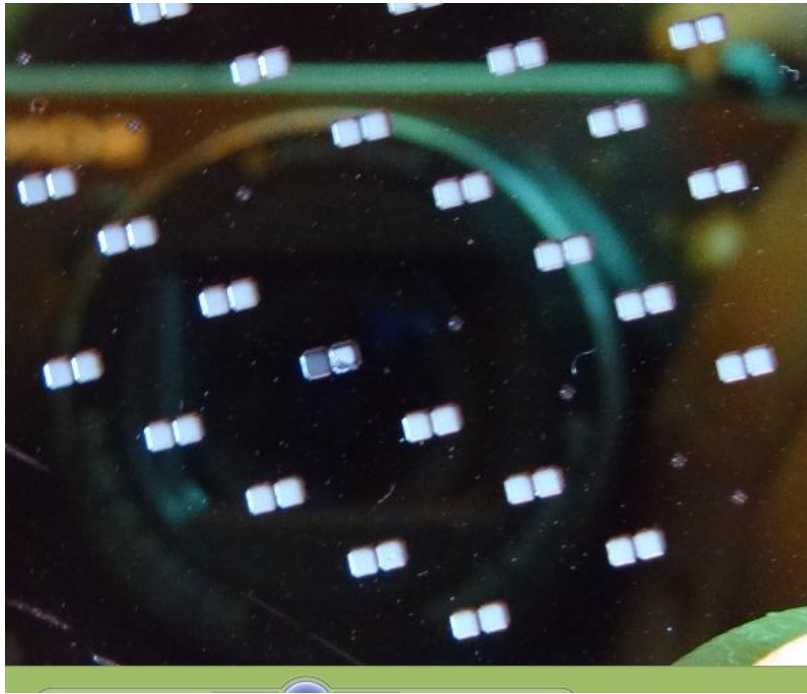


Fig.5.4 showing wafer after 1st etching step

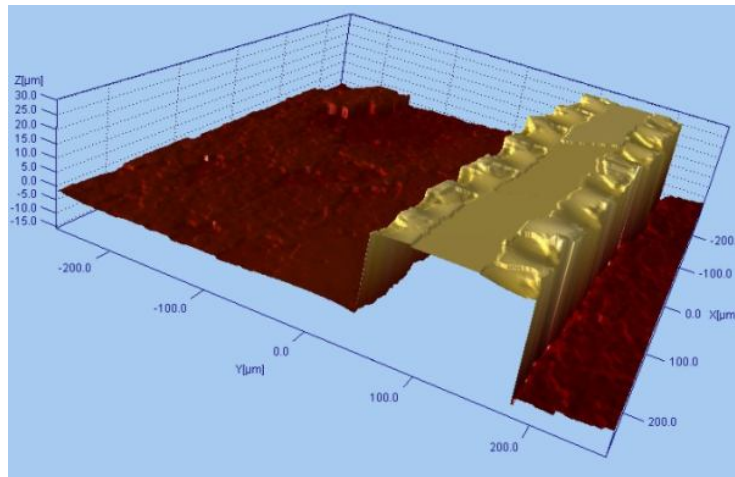


Fig. 5.5: The optical profilometry image of the etched pattern obtained where mask is in $\langle 100 \rangle$ direction



Fig. 5.6: Height and width of the etched pillar after first etching step.

Fig.5.

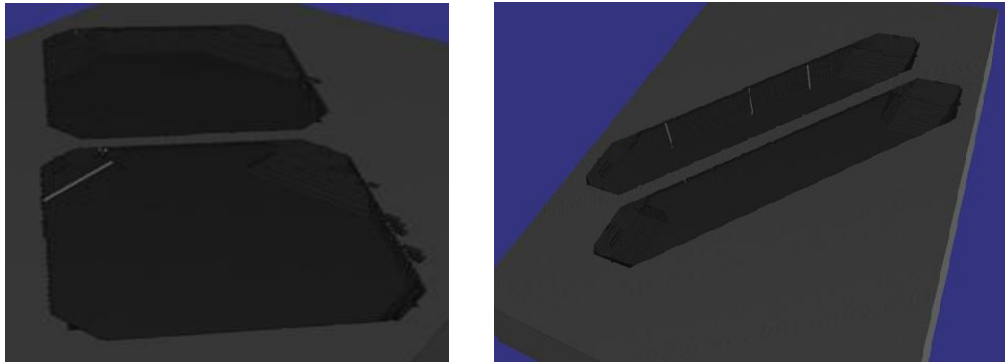


Fig.5.7.FABSIM based physical simulation for making Si micro bridge.

This is the most simple method of making Si microbridges by using only chemical etchant. But as we can observed from the result, for making we are wasting a lot of area being etched outside which is due to opening created by the mask. So to avoid this issue we go for some area efficient mask designs which is explained in the next section.

Chapter 6

Simulation and Fabrication of Si microbridges

6.1 Proposed Method to reduce area consumption for making Si Microbridges.

In the previous design the rectangular openings lead to high silicon area consumption which makes the process unworthy. Therefore we proposed different geometries to minimize area consumption for achieving the same dimension of suspended structure. All these different geometries are simulated using Intellisuite FABSIM based physical simulator. We have observed more than 28% reduction in foot print over literature reported design.

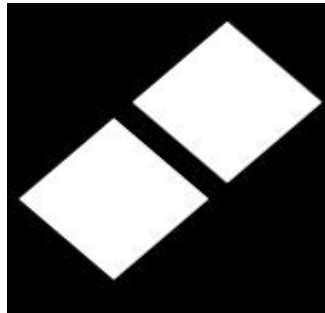


Fig.6.1 showing mask for basic microbridge obtained.

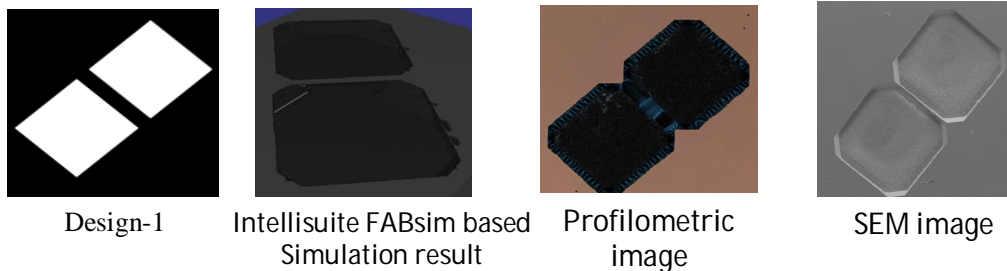
Fig.6.1 shows the mask used to create the Si micro bridge, where there are two rectangular openings. Those openings expose all the planes which are $\langle 100 \rangle$ in nature but out of all the $\langle 100 \rangle$ planes only one per opening is used to make the bridge. All other exposed $\langle 100 \rangle$ planes contributed to unnecessary etching outside the concerned area which increases foot print of each micro bridges. So to reduce the area consumed per device, we cut the mask used in previous case by half as shown in design-2. Now by doing this we have exposed only two $\langle 100 \rangle$ planes and one $\langle 111 \rangle$ plane which reduces the area consumed per pixel of Si bridge by more than half than the previous case.

Once again the area utilized per device can be reduced if we make the mask as shown in Design-3, where we reduced the openings for etchant to enter. But it can be observed from design-3 that, unnecessarily we are creating extra openings in the mask for the etchant where the device will not present. These areas can be saved if we cut half the portion of the mask as shown in Design-4. The mask gives advantage of opening only one $\langle 100 \rangle$ plane in the direction the device is present except which the etching in other directions is insignificant. This design is one of the most area efficient designs to make the Si micro bridges.

Another approach to minimize the area consumption per pixel also presented here. Where we halved each triangular opening shown in Design-2 in such a way that they will expose only one $\langle 100 \rangle$ plane and two $\langle 111 \rangle$ planes as shown in Design-5. As a result of which outside etching is prevented to happen because of $\langle 111 \rangle$ plane and there will be only inside etching due to $\langle 100 \rangle$ plane. Now if we want to reduce the area per pixel then we can go for the mask as shown in Design-6, where we reduced the opening for etchant to enter. Design-7 is made by bringing closer two same designs of category design-2. We are getting two advantages out of it. First all the outside planes are $\langle 111 \rangle$ in nature hence reduces underetch outside of concerned area and instead of getting only one microbridge, we are getting four microbridges. Now by design-8 we have reduced the opening for wet etchant which reduces area consumption further.

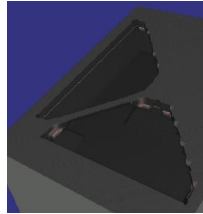
6.2 Simulation and Fabrication of Area efficient Si microbridges

We carried the FABSIM based physical simulation by considering all those masks which we put in fig.6.2. Each of the mask designs produce the same cantilever but the results obtained considering different mask designs gives a clear cut comparison of the area savings.

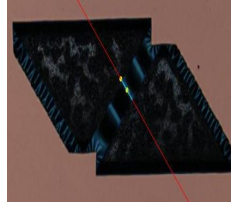




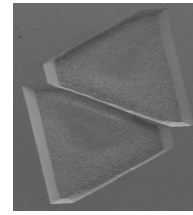
Design-2



Intellisuite FABSIm based Simulation result



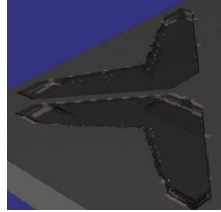
Profilometric image



SEM image



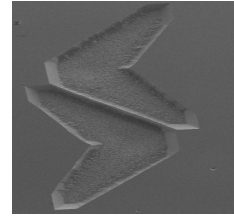
Design-3



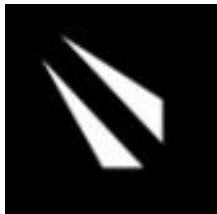
Intellisuite FABSIm based Simulation result



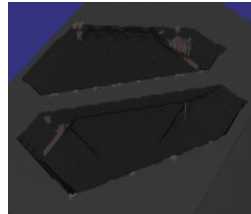
Profilometric image



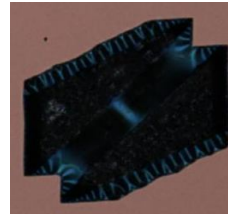
SEM image



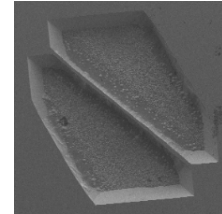
Design-4



Intellisuite FABSIm based Simulation result



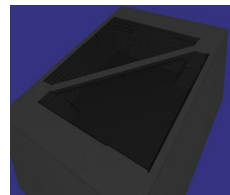
Profilometric image



SEM image



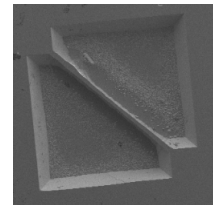
Design-5



Intellisuite FABSIm based Simulation result



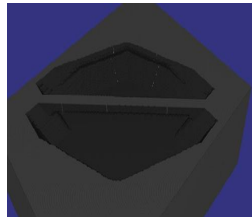
Profilometric image



SEM image



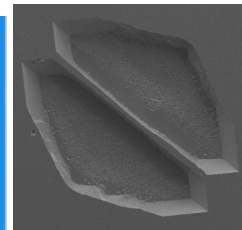
Design-6



Intellisuite FABSIm based Simulation result



Profilometric image



SEM image

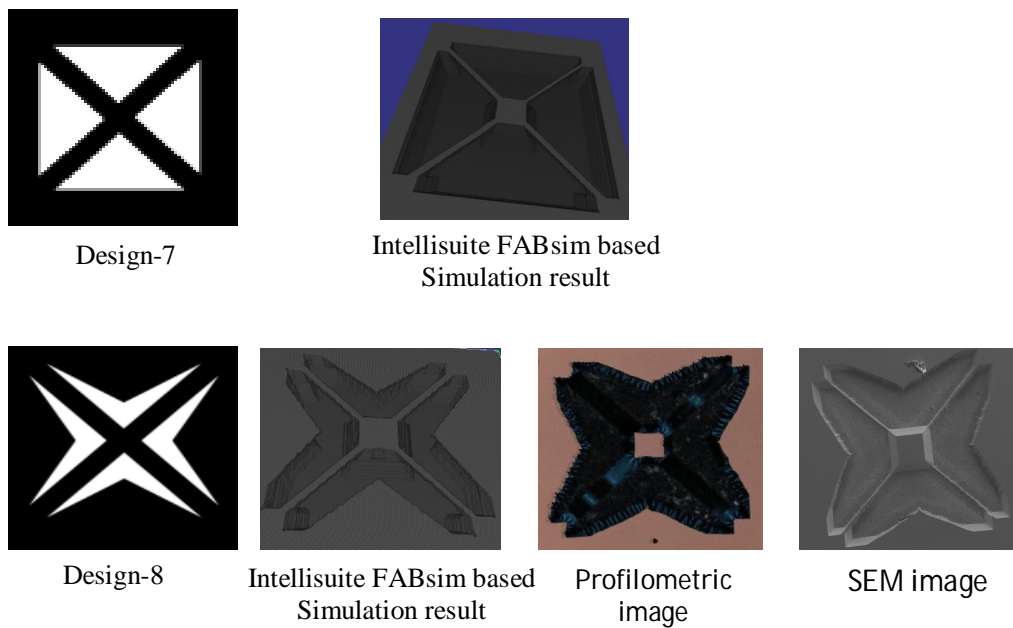


Fig.6.2: showing all the designs along with Intellisuit FABsim simulation , optical profilometry images and their corresponding SEM images.

The following fig.6.3 shows the cantilever beams. Where ater Si microbridges formed, by using another mask we etched the middle connecting island which gives rise to freely hanging isolated cantilever beams. This has implemented using mask design-7 and simulated using Intellisuit based FABsim physical simulator.

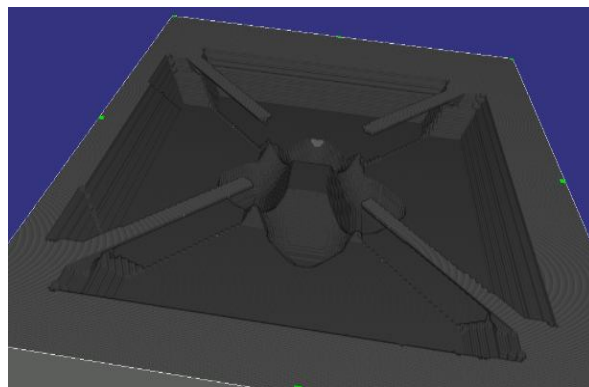


Fig.6.3: Showing cantilever beams through Intellisuit FABsim based physical simulation.

6.3 Comparative case study of the all area efficient mask Designs

Table-1 shows comparison of area consumption in making a microbridge and observed that almost 80% area saving as compare to basic design and about 28% as compared to design-4 which happened to be similar to Fang¹ reported design. Additionally we design and simulated four leg microbridge and four cantilevers by front end bulk micromachining by using the above mention concepts. This finding will be useful to fabricate cost effective and area effective different MEMS suspended structure in Si used in various sensors application.

TABLE-6.1

Showing the comparison of all the mask design presented

Designs	Opening area per mask	Outside Exposed <100> planes per mask	Number of beams generated	Total area consumed theoretically	Total area consumed from simulation (in sq. μm)	Remarks based on foot print per device
Design-1	A [#]	6	1	A+6 σ ^{\$}	111950	Poor
Design -2	A/2	2	1	A/2+2 σ	46326	Average
Design -3	A/2-2X*	2	1	A/2-2X+2 σ	37953	Good
Design -4	A/4	0	1	A/4	31708	Good
Design -5	A/4-X	0	1	A/4-X	25486	Very good
Design -6	A/4-X	0	1	A/4-X	22823	Very good
Design -7	A	0	4	A	29161	High
Design -8	A-4X	0	4	A-4X	22141	Excellent

[#]=Opening area per mask, ^{*}(X= saved area per opening), ^{\$}=etch in <100> plane

Chapter 7

Microbolometer and Design

7.1 Innovative method for fabricating Microbolometer

A lot of techniques have been reported so far to fabricate microbolometers and array of it. But all the methods reported have certain drawbacks e.g. pixel form factor, cost and temperature. We are reporting a technique in which the silicon itself is a bolometer sensing material as that in the case of CMOS line bolometer but unlike CMOS type, here the same silicon substrate is used as the sensing material, may be n-type or p-type depending on the substrate we have chosen, hence avoiding the diffusion step which is required for etch stopping in standard CMOS line bolometer. We are targeting to achieve the array of bolometer by 3D integration technique unlikely that of usual 3D integration where a sacrificial layer is required which may suffer from the reliability issue of being the hanging structure.

Here we are reporting an innovative way of fabricating Bolometer device only by front end bulk micromachining where neither diffusion nor the cumbersome electrochemical etch stopping is required. The thermally insulated membrane achieved can be used as the bolometer sensing material and if we want to increase the sensitivity we can deposit any of the high TCR material such as VO_x over the membrane before going for 3D integration with the ROIC. As the membrane itself is the part of the silicon substrate it is going to give much better reliability as compared to the recently developed heterogeneous 3D integration of bolometer.

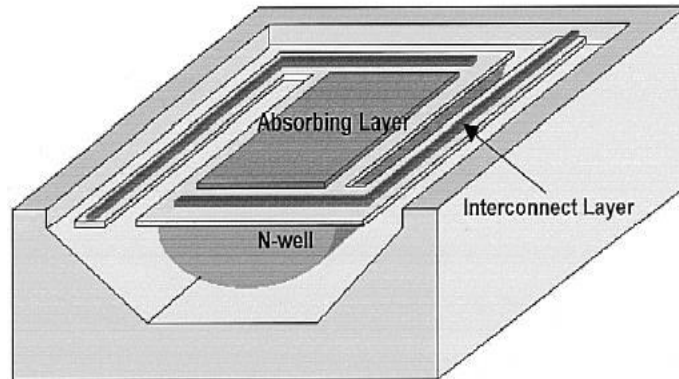


FIG.7.1: showing the standard CMOS line Bolometer fabrication where n-well is used as the sensing layer.

7.2 Process Simulation showing Microbolometer Fabrication using only Front end Bulk micromaching

We adopted mainly two fabrication processes for microbolometer sensor . One involving only wet etching of Si and in the other, dry etching followed by wet etching. Here we are reporting both the processes. In either of the method we started with oxidised Si wafers. Made the desired mask for bolometer sensor and rotated it by 45° before printing as the primary step. Every part of the mask is nothing but a rectangular structure, so rotating it with 45 degree and putting in TMAH will result in vertical etching , as all the $\langle 100 \rangle$ planes are exposed inside.

7.2.1 Only using wet etching

Fabrication using only chemical etching started with a mask dimension of 128 μm length and 60 μm width. To make the process more cost effective only one mask is used in the entire process. At first we exposed the spin coated Si wafer with the mask and etched for 9000nm. Then the resulting etched wafer is put in oxidation chamber to get oxidized. As the TMAH etching is done both in horizontal as well as vertical direction, etching started exposing the $\langle 111 \rangle$ planes as it goes in horizontally, those exposed $\langle 111 \rangle$ planes created problem by restricting etching in that direction. So we have broken these exposed $\langle 111 \rangle$ planes using isotropic etchant HNA ($\text{HNO}_3 + \text{HF}$) by going to a depth of 7600nm. After isotropic etching the wafer is cleaned and then again oxidized. Now in the final step the resulting etched Si wafer is again etched using anisotropic wet etchant TMAH, which

results in the formation of freely standing isolated membrane which can be used as the sensor for microbolometer. In the whole process we have used only one mask for exposing under UV. The process flow of the above method is shown in the fig.7.2.

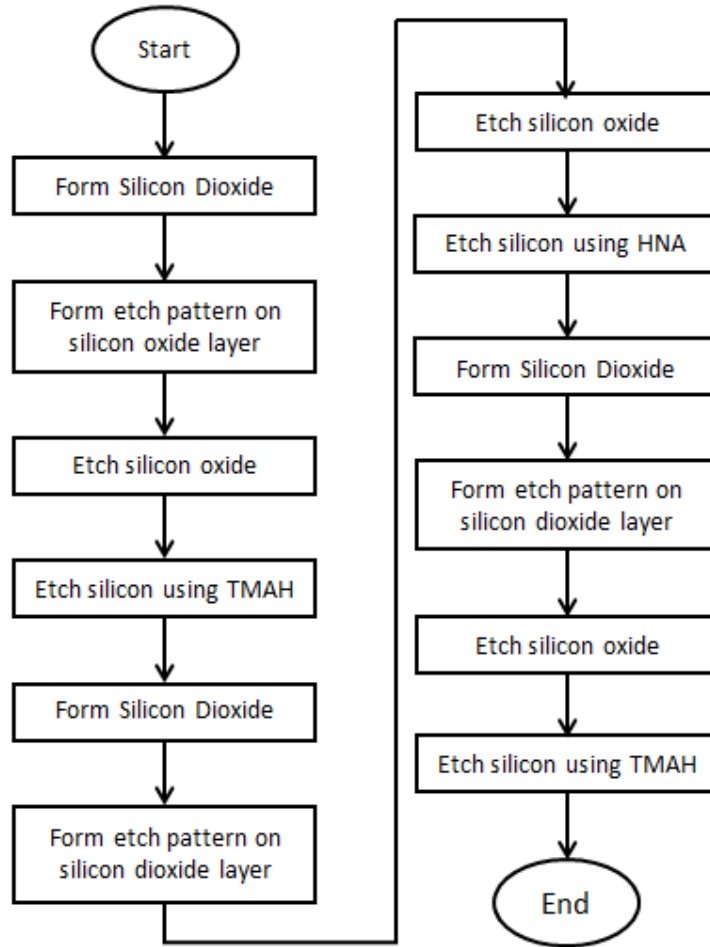


Fig.7.2: showing process flow to obtain microbolometer sensor.

7.2.1.1 Simulation Results

The above process is simulated using Intellisuite FABSIM based physical simulator. Fig.7.3 shows the basic mask design used for the above method and simulation result showing sensor membrane. Fig.7.4 shows the process table used to make the above sensor membrane.



Fig.7.3: showing the mask used and the bolometer sensor membrane obtained using Intellisuite based FABSIm physical simulation.

1	Definition	Si	Czochralski	100	
2	Etch	Si	Clean	RCA	
3	Deposition	SiO2	Thermal	Wet	Conformal Deposition
4	Etch	Si	Clean	RCA	
5	Etch	Si	Clean	Piranha	
6	Deposition	PR-S1800	Spin	SI813	Conformal Deposition
7	Exposure	UV	Contact	Suss	
8	Etch	SiO2	Wet	BHF	Partial Etching
9	Etch	PR-S1800	Wet	1112A	Partial Etching
10	Etch	Si	Wet	TMAH	Partial Etching
11	Etch	SiO2	Wet	BHF	Partial Etching
12	Etch	Si	Clean	Piranha	
13	Deposition	SiO2	Thermal	Wet	Conformal Deposition
14	Etch	Si	Clean	RCA	
15	Etch	Si	Clean	Piranha	
16	Deposition	PR-S1800	Spin	SI813	Conformal Deposition
17	Exposure	UV	Contact	Suss	
18	Etch	SiO2	Wet	BHF	Partial Etching
19	Etch	PR-S1800	Wet	1112A	Partial Etching
20	Etch	Si	Wet	TMAH	Partial Etching
21	Etch	Si	Wet	HNO3_HF	Partial Etching
22	Etch	SiO2	Wet	BHF	Partial Etching
23	Etch	Si	Clean	Piranha	
24	Deposition	SiO2	Thermal	Wet	Conformal Deposition
25	Etch	Si	Clean	RCA	
26	Etch	Si	Clean	Piranha	
27	Deposition	PR-S1800	Spin	SI813	Conformal Deposition
28	Exposure	UV	Contact	Suss	
29	Etch	SiO2	Wet	BHF	Partial Etching
30	Etch	PR-S1800	Wet	1112A	Partial Etching
31	Etch	Si	Wet	TMAH	Partial Etching
32	Etch	SiO2	Wet	BHF	Partial Etching
33	Etch	Si	Clean	Piranha	

Fig.7.4: showing process table for the above method.

7.2.2 Dry etching followed by Wet etching

7.2.2.1 DRIE followed by TMAH etching

In this method of making microbolometer sensor, dry etching was adopted in the 1st step which was DRIE (deep reactive ion etching) then wet etching was carried out using TMAH. We started with the mask for targeting to make microbolometer sensor of dimension 20 μ mX20 μ m and length of the sensor as 5 μ m. The 1st etching step was done to a depth of

10 μm by using DRIE and the 2nd etch step to a depth of around 15 μm by using anisotropic wet etchant TMAH. Because of the mask orientation, TMAH etch in horizontal direction along with vertical giving freely hanging and isolated Si membrane which can be used as microblometer sensor. Here we have used two masks for making the sensor membrane unlike of the previous method, where one is used for creating opening for dry etching and second for creating opening for wet etching. Fig.7.5 shows the process flow to obtain microbolometer using above method.

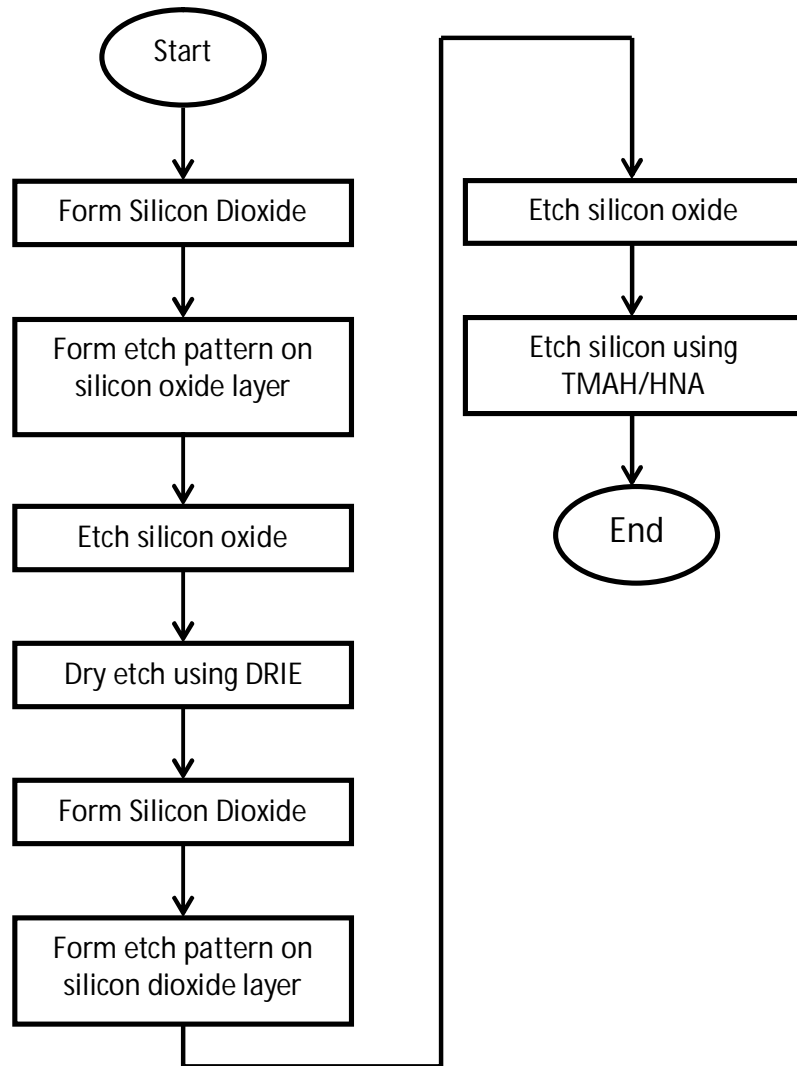


Fig.7.5: shows process flow to obtain Microbolometer using above method.

7.2.2.1.1 Simulation results

The above process is simulated using Intellisuite FABSIm based physical simulator. Fig.7.6 shows the mask used for the above method, simulation result showing sensor membrane and fig.7.7 shows the process table used to make the above sensor membrane.

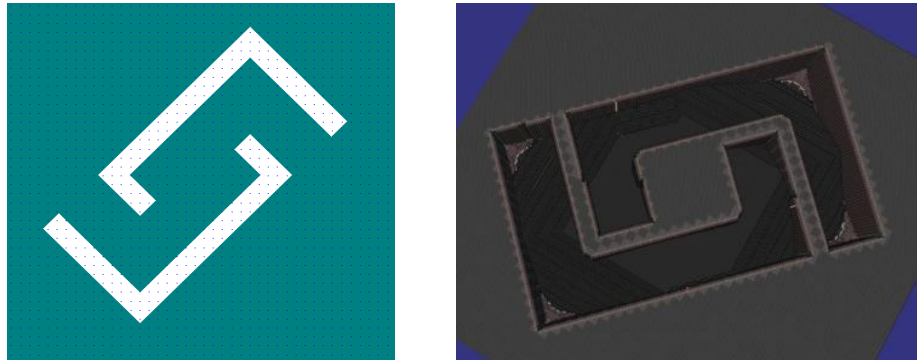


Fig.7.6: showing the mask used and the bolometer sensor membrane obtained using Intellisuite based FABSIm physical simulation.

1	Definition	Si	Czocharlski	100	
2	Etch	Si	Clean	RCA	
3	Deposition	SiO2	Thermal	Wet	Conformal Deposition
4	Etch	Si	Clean	RCA	
5	Etch	Si	Clean	Piranha	
6	Deposition	PR-S1800	Spin	S1813	Conformal Deposition
7	Exposure	UV	Contact	Suss	
8	Etch	SiO2	Wet	BHF	Partial Etching
9	Etch	PR-S1800	Wet	1112A	Partial Etching
10	Etch	Si	DRIE	SF6_c4F8	Partial Etching
11	Etch	SiO2	Wet	BHF	Partial Etching
12	Etch	Si	Clean	Piranha	
13	Deposition	SiO2	Thermal	Wet	Conformal Deposition
14	Etch	Si	Clean	RCA	
15	Etch	Si	Clean	Piranha	
16	Deposition	PR-S1800	Spin	S1813	Conformal Deposition
17	Exposure	UV	Contact	Suss	
18	Etch	SiO2	Wet	BHF	Partial Etching
19	Etch	PR-S1800	Wet	1112A	Partial Etching
20	Etch	Si	Wet	TMAH	Partial Etching
21	Etch	SiO2	Wet	BHF	Partial Etching
22	Etch	Si	Clean	Piranha	

Fig.7.7: showing process table for the above method.

7.2.2.2 DRIE followed by HNA etching

This method is similar to that of previous method except of using isotropic etchant HNA instead of anisotropic etchant TMAH in the 2nd etching step.

7.2.2.2.1 Simulation Results

The above process is simulated using Intellisuite FABsim based physical simulator. The below fig.7.8 shows the mask used for the above method, simulation result showing sensor membrane and the process table used to make the above sensor membrane.



Fig.7.8: showing the mask used and the bolometer sensor membrane obtained using Intellisuite based FABsim physical simulation

Chapter 8

Efficient Method to Fabricate Microbolometer

8.1 Design and Simulation of area efficient Microbolometers

The mask used in the previous chapter to make the microbolometer sensor is made up of all rectangular areas which when exposed on Si wafer will open all the $\langle 100 \rangle$ planes inside as well as outside. Due to which we will not only have undercut inside but also will lose area outside which needs to be prevented. More the area consumed by the sensor, less will be the pixel fill factor. So to reduce the area consumption, we have made some designs which will allow the etchant to enter only in the desired direction and prevent unnecessary area consumption in all other directions. Those mask designs are useful in both the methods of fabricating the microbolometer sensor, which has been described neatly in the below subsections. We have proposed around four mask designs to reduce the area consumed per pixel of microbolometer sensor. The same concept has been applied to make an area-efficient microbolometer, as that of making an area-efficient Si microbridge. Below are the explanations of all mask designs.

Design-1 :

This is the basic mask design used to make a microbolometer sensor. The openings in this design are all rectangular in nature.

Design-2 :

The mask area opened for etchant in Design-1 can be reduced by cutting down, as shown in the figures. As in Design-2, the area of opening is reduced to half of that of Design-1, so area consumption due to outside etching is also reduced.

Design-3 :

In this design, we replace the rectangularly opened mask by a number of elemental right-angled triangular structures. While rotating the mask by 45° , the sides of each triangle will expose $\langle 111 \rangle$ planes and the hypotenuse will expose $\langle 100 \rangle$ plane. Hence, the etching in outside will be reduced significantly.

Design-4 :

In this design we cut the rectangular region in Design-1 into triangular region as shown in the figure. The mentioned design is also helpful in saving area due to outside etching.

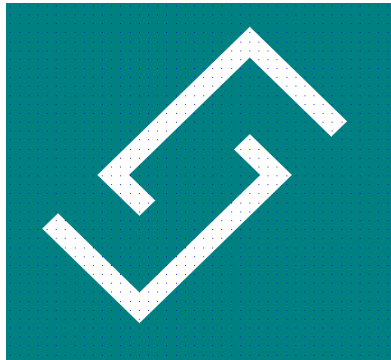
Design-5 :

In this design instead of one triangle as in Design-4 we are going for two triangular regions as shown in the figure. This also helpful in reducing area consumption due to outside etching.

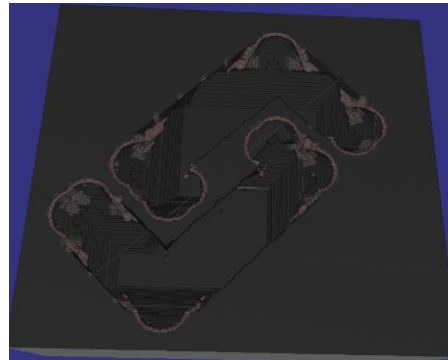
Below presented all the mask designs with their corresponding Intellisuite based Fabsim simulation results.

8.1.1 Only using wet etching

As in previous chapter in this method we are going to use only wet chemical etchants to make microbolometer sensors. Fig.8.1 shows the Designs with corresponding simulation results to obtain microbolometer sensor and table showing length and width per each pixel.



Design-1



Simulation result in Fabsim

Measure Result	
Absolute Distance :	150.212 um
Vertical Distance :	0.206524 um
Horizontal Distance :	150.212 um
Elevation Angle :	0.0787751 deg

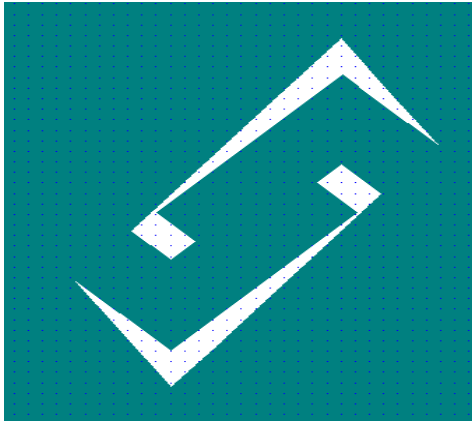
Start Measure OK

Length of the pixel

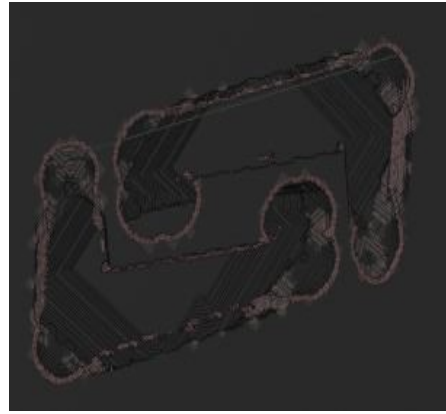
Measure Result	
Absolute Distance :	80.5221 um
Vertical Distance :	1.07596 um
Horizontal Distance :	80.5149 um
Elevation Angle :	0.785554 deg

Start Measure OK

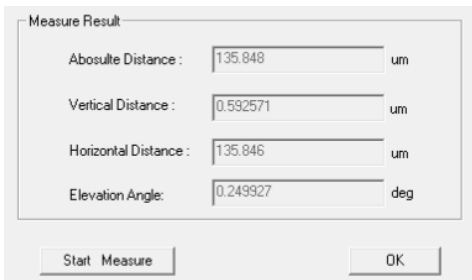
Width of the pixel



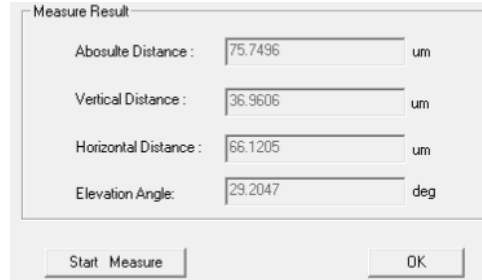
Design-2



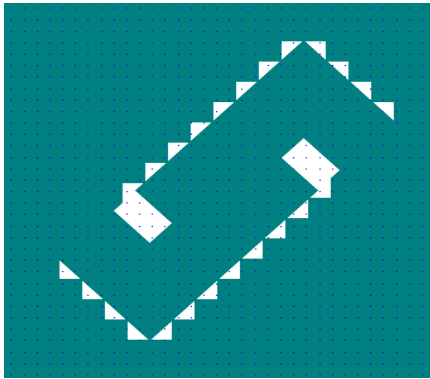
Simulation result in Fabsim



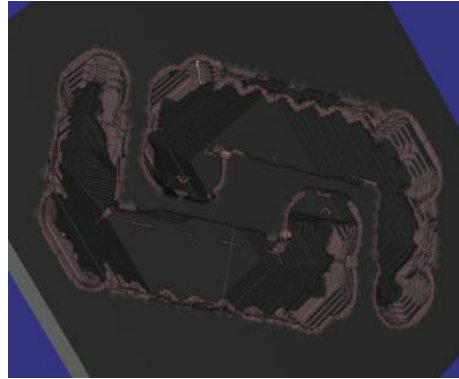
Length of the pixel



Width of the pixel



Design-3



Simulation result in Fabsim

Measure Result

Absolute Distance : um

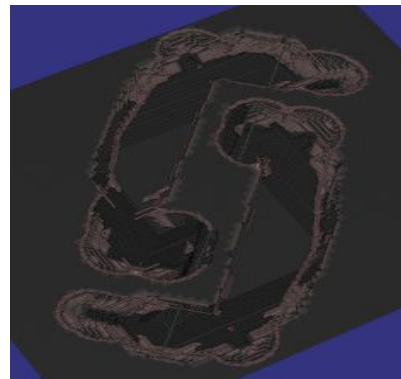
Vertical Distance : um

Horizontal Distance : um

Elevation Angle: deg



Design-4



Simulation result in Fabsim

Measure Result

Absolute Distance : um

Vertical Distance : um

Horizontal Distance : um

Elevation Angle: deg

Length of the pixel

Measure Result

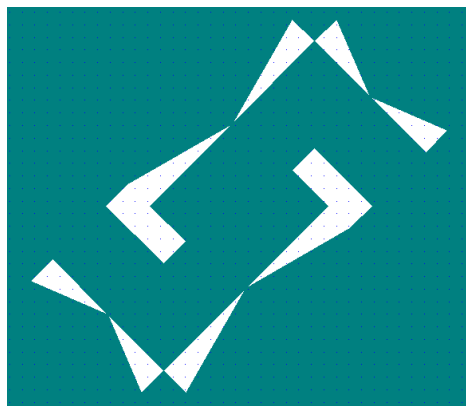
Absolute Distance : um

Vertical Distance : um

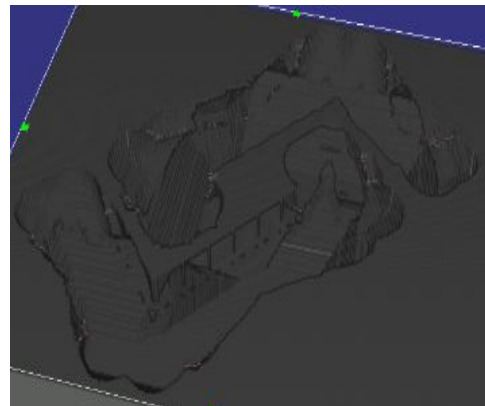
Horizontal Distance : um

Elevation Angle: deg

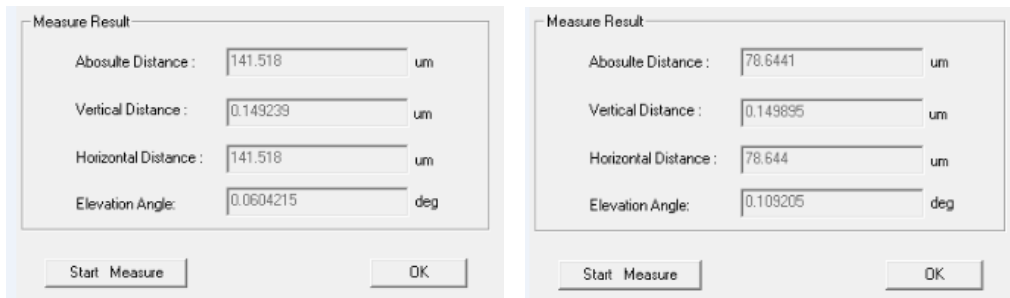
Width of the pixel



Mask design- 6



Simulation result in Fabsim



Length of the pixel

Width of the pixel

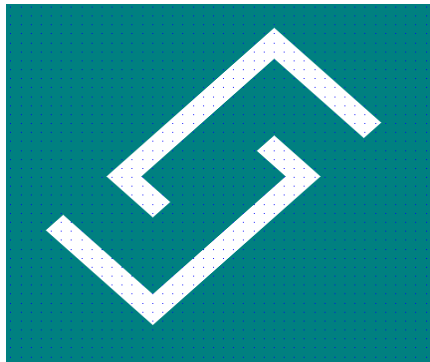
Fig.8.1: shows different designs with their corresponding Simulation results in Intellisuite FABSIm based physical simulator for above method.

8.1.2 Dry etching followed by Wet etching

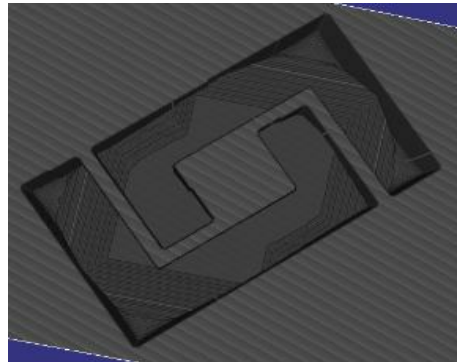
As in the previous chapter here in this method also we are going for dry etching 1st and next wet etching but with different mask designs. In the subsequent sections we put simulation results for both the sub methods under the mentioned method for all the five mask designs.

8.1.2.1 DRIE followed by TMAH etching

Below fig.8.2 shows all the designs with their corresponding simulation results.



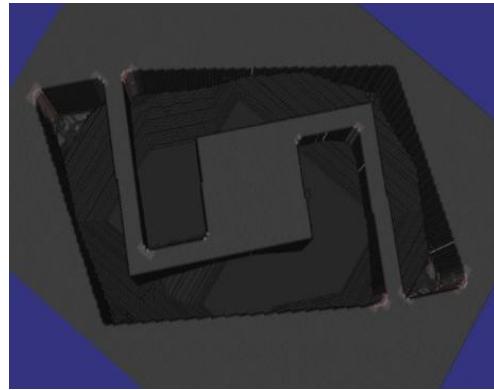
Mask design- 1



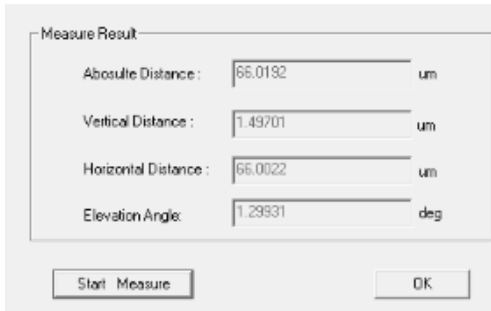
Simulation result in Fabsim



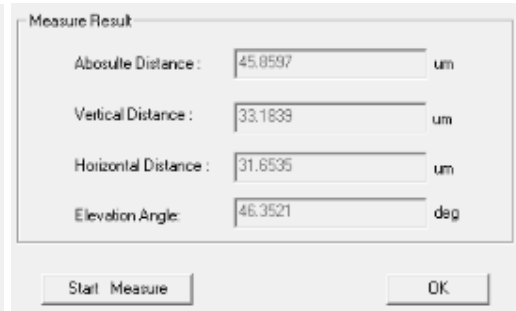
Mask design- 2



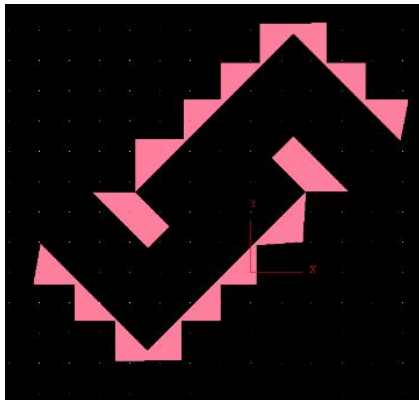
Simulation result in Fabsim



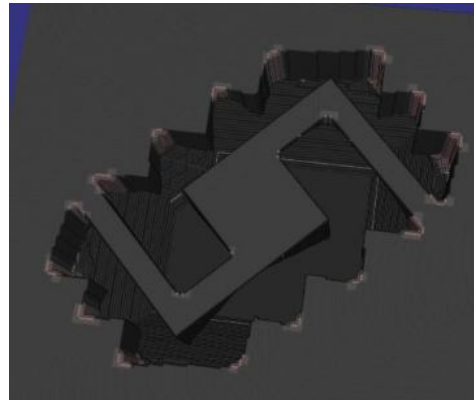
Length of the pixel



Width of the pixel



Mask design- 3



Simulation result in Fabsim

Measure Result

Absolute Distance : um

Vertical Distance : um

Horizontal Distance : um

Elevation Angle : deg

Length of the pixel



Mask design- 4

Measure Result

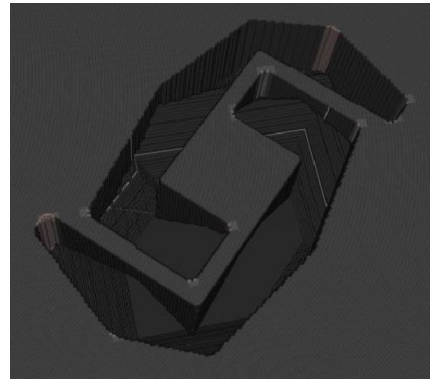
Absolute Distance : um

Vertical Distance : um

Horizontal Distance : um

Elevation Angle : deg

Width of the pixel



Simulation result in Fabsim

Measure Result

Absolute Distance : um

Vertical Distance : um

Horizontal Distance : um

Elevation Angle : deg

Length of the pixel



Mask design-5

Measure Result

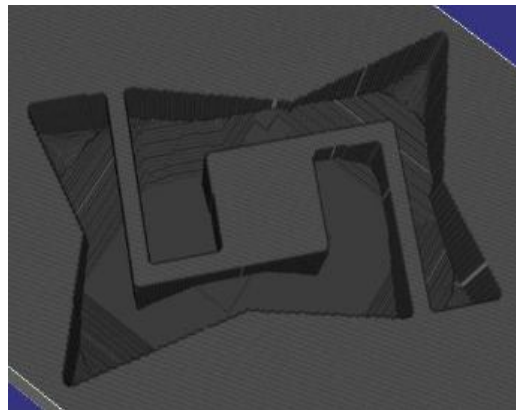
Absolute Distance : um

Vertical Distance : um

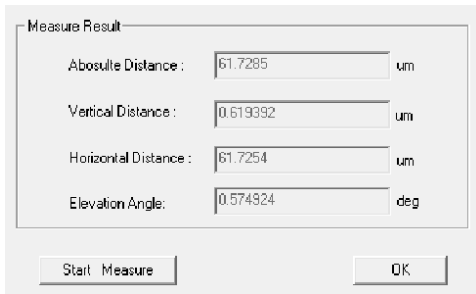
Horizontal Distance : um

Elevation Angle : deg

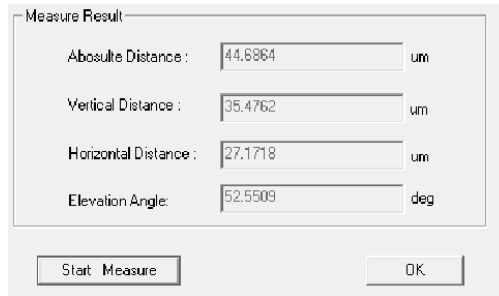
Width of the pixel



Simulation result in Fabsim



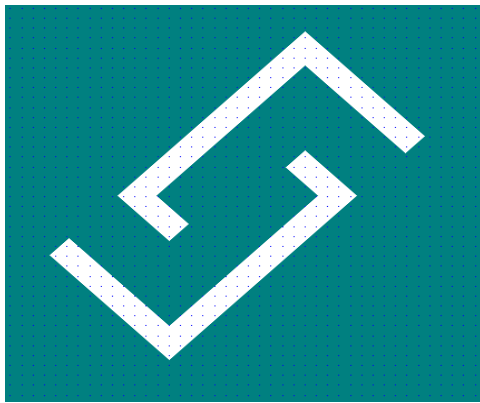
Length of the pixel



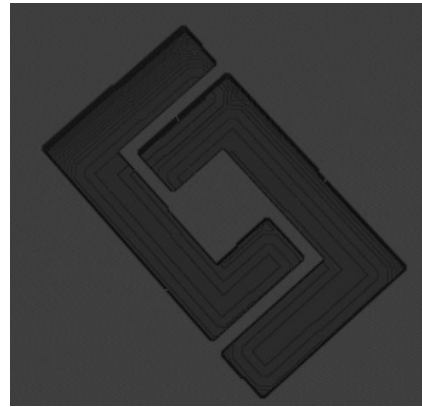
Width of the pixel

Fig.8.2: shows different designs with their corresponding Simulation results in Intellisuite FABsim based physical simulator for above method.

8.1.2.2 DRIE followed by HNA etching



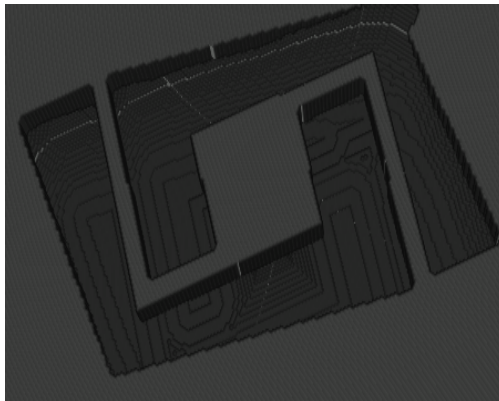
Mask design-1



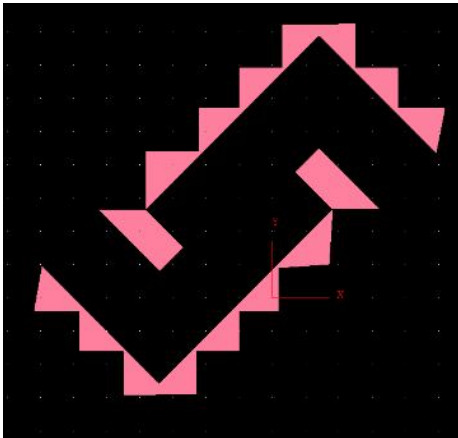
Simulation result in Fabsim



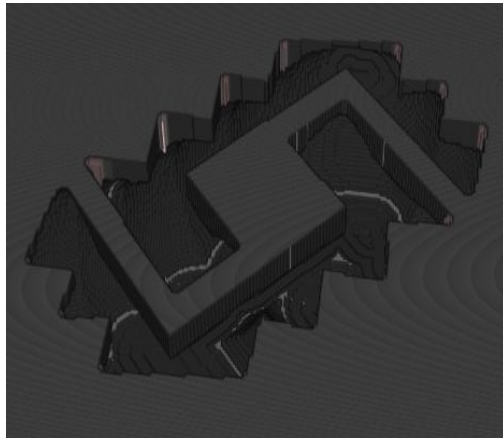
Mask design-2



Simulation result in Fabsim



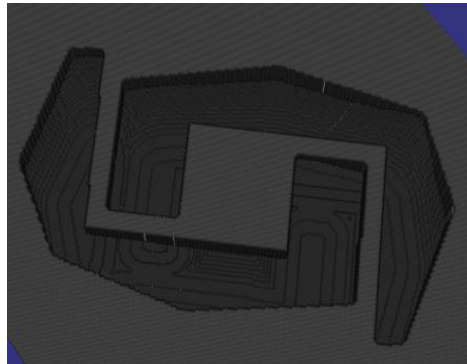
Mask design-3



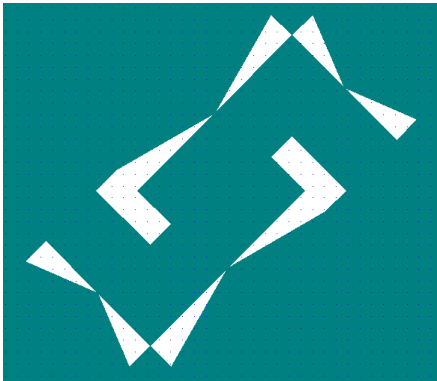
Simulation result in Fabsim



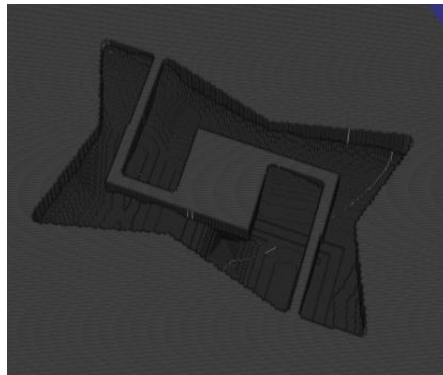
Mask design-4



Simulation result in Fabsim



Mask design-5



Simulation result in Fabsim

Fig.8.3: shows different designs with their corresponding Simulation results in Intellisuite FABSIm based physical simulator for above method.

In this case we have observed length and width calculated per pixel are same as that of the previous method i.e. DRIE followed by TMAH etching. Hence the table showing length and width of pixel is not explicitly put here. The area per each pixel is dependent on DRIE step which actually depends on the dimension of mask used in the 1st etching step. So in this method the area of each pixel of microbolometer sensor is almost equal to the area designed for mask in the 1st etching step.

Chapter 9

Comparative case study of Making Microbolometer Sensor

9.1 Comparisons between only wet etching and dry followed by wet etching

- In the 1st method of fabricating the device we have used only one mask and isotropic and anisotropic wet etchants for making the detector which results in low cost method of fabricating the device.
- But the process is somewhat complicated being controlled by the time of etching and depth of etching and the second thing we have started with 128umX60um pixel of mask and should expect the device of same size but taking the advantage of horizontal etching results in the increase in pixel dimension, due to which the device consumed an area of 150umX80um. So we need to consume some significant amount area in fabricating microbolometer sensor in this method. So the pixel fill factor is not pretty good.
- In the 2nd method of fabricating the device which required two masks and DRIE makes the process more costly as compared to the previous process.
- But it gives certain advantages because the TMAH etching is required only in the 2nd etching step where the timing of etching and depth is not that stringent as that of 1st method where we have taken care of time of etching and etch depths in all of the three etching steps and optimized that. Secondly if we target for the dimension of device i.e. 128umX60um then we will be having pixel area of that much only as the important step is the 1st etching step in terms of area consumed per pixel taken care by DRIE hence not allowing any other direction of etching except in vertical.

Table-9.1 shows the calculation and comparisons of area calculated of all the methods of fabricating microbolometers for all the designs.

Table-9.1 showing area calculate for microbolometer fabrication using all the designs

	Area per pixel using Method1(μm^2)	Area per pixel using Method2-sub method-1(μm^2)	Area per pixel using Method2-sub method-2(μm^2)
Design1	12095	2800	2800
Design2	10290	2090	2090
Design3	10080	2515	2515
Design4	9105	2574	2574
Design5	11130	1684	1684

9.2 Comparisons between sub methods under method-2

Comparing the two processes under dry followed by wet etching, we observed using HNA in 2nd step of etching consumes more area inside the bulk Si as compared of using TMAH in 2nd step. Below fig.9.1 shows the simulated result showing the maximum distance etched by both the processes. Where it is easily visible HNA is consuming more area as compared of using TMAH for the same mask.

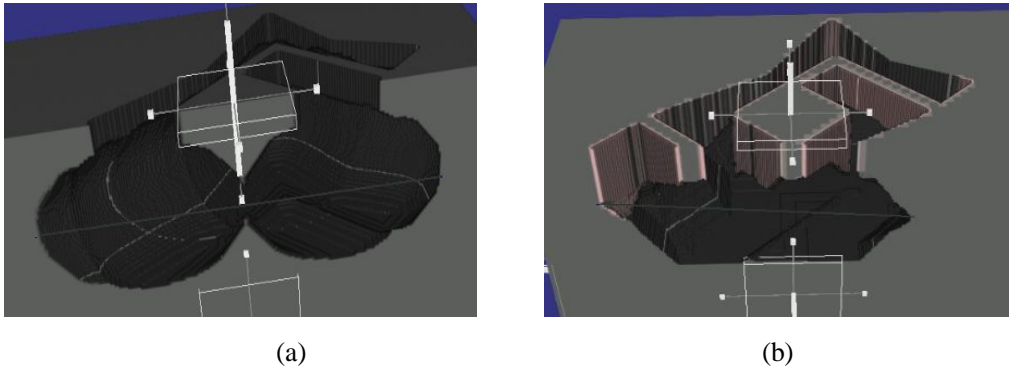


Fig.9.1: (a) shows under etch inside bulk Si using HNA and (b) shows under etch inside bulk Si using TMAH.

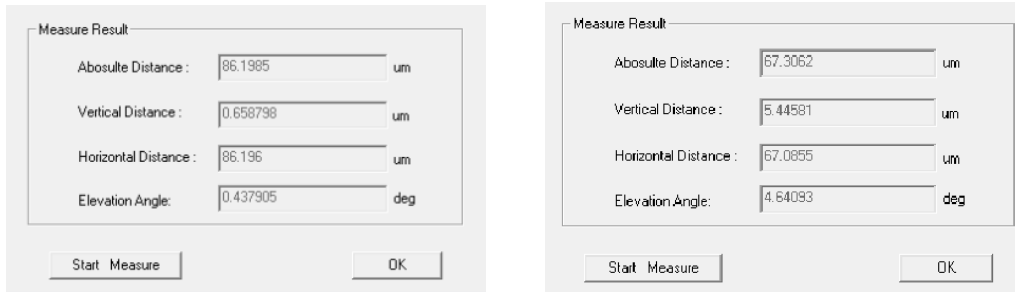


Fig.9.2: (a) shows the table calculating maximum distance etched under bulk Si using HNA and (b) shows maximum distance etched inside bulk Si using TMAH.

9.3 Comparisons between proposed methods and existing methods of making microbolometer sensor

Table below shows comparisons between the existing methods of fabricating microbolometer and proposed methods.

Table-9.1 shows comparison between existing method and proposed method to fabricate microbolometer sensor.

METHODS	COST	RELIABILITY	EASE	SENSING
CMOS line	LOW	HIGH	MODERATE	MODERATE
HETEROGENEOUS 3D INT.	HIGH	LOW DUE TO HANGING STRUC TURE	DIFFICULT	High
PRESENT METHODS	LOW-method-1 Moderate Method-2	HIGH as Si is the part of the substrate In both methods	MODERATE	MODERATE if used in cmos line high if in heterogeneous 3D with VOx

Chapter 10

Conclusion and Future Work

10.1 Conclusion

In the present work we have proposed cost effective and novel way to make microbolometer sensor as well as Si microbridges. Where the proposed method of making Si Micro bridges or cantilever beams is based on simple wet etching technique i.e. the frontend bulk micromachining which reduces the requirement of clean room and hence the cost associated with it. The efficient mask designs proposed decreases foot print of individual pixels hence increases overall efficiency of the device which may be simple Si micro bridge or cantilever or any of the complicated structure or may be array of any of the above.

The methods proposed in the work to fabricate microbolometer sensor are simple and majorly consists of etching steps only. These methods doesn't require any diffusion or electrochemical etch stopping technique, which may complicate the process, rather the simple wet etching steps avoids the requirement of clean room which can reduce the cost of making the device specially the method 1 way of fabricating microbolometer sensor.

10.2 Future Scope of Work.

The present work was focused to make microbolometer sensor in a simple and cost effective way. The scope for the future work is listed below.

- Fabrication and characterization of the microbolometer sensor.
- Deposition of high TCR microbolometer sensing material e.g. VO_x to increase sensitivity of the device.
- Mirror material deposition at bottom of the sensor for capturing more IR radiations.
- 3D integration of microbolometer sensor with its corresponding ROIC.

References

- [1] GREGORY T. A. KOVACS, MEMBER, IEEE, NADIM I. MALUF, MEMBER, IEEE, AND KURT E. PETERSEN, FELLOW, IEEE “Bulk Micromachining of Silicon” PROCEEDINGS OF THE IEEE, VOL. 86, NO. 8, AUGUST 1998.
- [2] Frank Niklaus, Christian Vieider, Henrik Jakobsen” MEMS-Based Uncooled Infrared Bolometer Arrays – A Review” MEMS/MOEMS Technologies and Applications III, III, edited by Jung-Chih Chiao, Xuyuan Chen, Zhaoying Zhou, Xinxin Li, Proc. of SPIE Vol. 6836, 68360D, (2007).
- [3] Selim Eminoglu, Deniz Sabuncuoglu Tezcan, M. Yusuf Tanrikulu, Tayfun Akin “Low-cost uncooled infrared detectors in CMOS process” *Department of Electrical and Electronics Engineering, Middle East Technical University, Ankara 06531, Turkey*. Sensors and Actuators A 109 (2003) 102–113.
- [4] Deniz Sabuncuoglu Tezcan*, Selim Eminoglu", Orhan Sevket Akar**, and Tayfun .Akin*, * Department of Electrical and Electronics Engineering, Middle East Technical University, *Ankara*, Turkey “A LOW COST UNCOOLED INFRARED MICROBOLOMETER FOCAL PLANE ARRAY USING THE CMOS N-WELL LAYEIR”*** TUBITAK-BILTEN, Middle East Technical University, Ankara, Turkey.
- [5] BEN KLOECK, SCOTT D. COLLINS, NICO F. DE ROOIJ, AND ROSEMARY L. SMITH “Study of Electrochemical Etch-Stop for High-Precision Thickness Control of Silicon Membranes”, IEEE TRANSACTIONS ON ELECTRON DEVICES. VOL. 36. NO. 4. APRIL 1989.
- [6] Frank Niklaus, Adit Decharat, Fredrik Forsberg , Niclas Roxhed , Martin Lapisa, Michael Populin ,Fabian Zimmer, Jörn Lemmb, Göran Stemme “Wafer bonding with nano-imprint resists as sacrificial adhesive for fabrication of silicon-on-integrated-circuit (SOIC) wafers in 3D integration of MEMS and ICs” Sensors and Actuators A 154 (2009) 180–186.
- [7] BEN KLOECK, SCOTT D. COLLINS, NICO F. DE ROOIJ, AND ROSEMARY L. SMITH “Study of Electrochemical Etch-Stop for High-Precision Thickness Control of Silicon Membranes” IEEE TRANSACTIONS ON ELECTRON DEVICES. VOL. 36. NO. 4. APRIL 1989.
- [8] Ei-no H. Klaassen *, Richard J. Reay, Christopher Storment, Gregory T.A. Kovacs Center fi-r btegrated Systems. CIS-X 202. Stanford Univerm~'. Stanford, CA 94305-4075 USA “Micromachined thermally isolated circuits” Sensors and Actuators A 58 (1997) 43-50.
- [9] M.C. Acero, J. Esteve, Chr.Burrer, A. Gotz ”Electrochemical etch-stop characteristics of TMAH:IPA solutions “ Sensors and actuators A46-47(1995) 22-26.
- [10] Ernest Bassous “Fabrication of novel Three- Dimensional microstructures by anisotropic etching of (100) and (110) Silicon” IEEE Transactions on Electron Devices, Vol. ED-25, NO.10 October 1978.
- [11] E.chen Applied physics 298r.
- [12] Frank Niklaus, Adit Decharat, Fredrik Forsberg , Niclas Roxhed , Martin Lapisa, Michael Populin ,Fabian Zimmer, Jörn Lemmb, Göran Stemme “Wafer bonding with nano-imprint resists as sacrificial adhesive for

- fabrication of silicon-on-integrated-circuit (SOIC) wafers in 3D integration of MEMS and ICs" *Sensors and Actuators A* 154 (2009) 180–186.
- [13] Weileun Fang "Design of bulk micromachined suspensions" *J. Micromech. Microeng.* **8** (1998) 263–271.

